

Glycomic and Glycoproteomic Analysis of Serum from Patients with Stomach Cancer Reveals Potential Markers Arising from Host Defense Response Mechanisms

Jonathan Bones,[†] Jennifer C. Byrne,^{†,‡} Niaobh O'Donoghue,[†] Ciara McManus,[†] Caitriona Scaife,[§] Herve Boissin,^{||} Anca Nastase,^{||} and Pauline M. Rudd^{*,†}

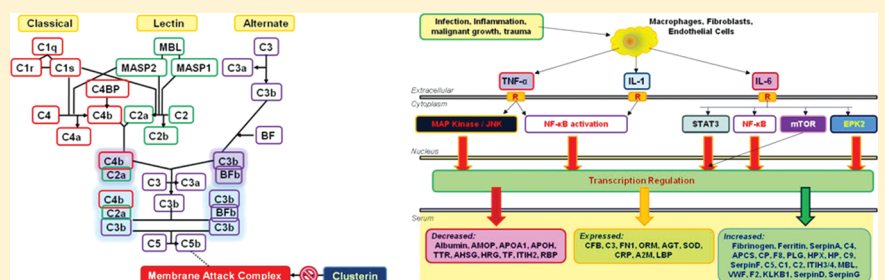
[†]NIBRT Dublin-Oxford Glycobiology Laboratory, The National Institute for Bioprocessing Research and Training and [§]Proteome Research Centre, UCD Conway Institute of Biomolecular and Biomedical Research, University College Dublin, Belfield, Dublin 4, Ireland

[†]Molecular and Cellular Therapeutics, Royal College of Surgeons in Ireland, 123 St. Stephen's Green, Dublin 2, Ireland

^{||}RNTech SAS France, Rue Tronchet 8, 75008 Paris, France

ABSTRACT: Despite the reduced incidence of gastric cancer in the developed world, a diagnosis of stomach carcinoma still carries a poor prognosis due to the asymptomatic nature of the disease in the early stages, subsequent advanced stage diagnosis, and a low 5 year survival rate. Endoscopy remains the primary standard for diagnosis of stomach carcinoma and the current marker, carbohydrate antigen 19-9 (CA19-9) lacks the levels of sensitivity and specificity required in order to make it clinically useful for diagnostic monitoring. Therefore, there is a current need for additional markers to improve the diagnostic accuracy for the early stages of stomach cancer. Together, glycomic, proteomic, and glycoproteomic analyses of serum have the potential to identify such probable markers. A discovery study is reported here using preoperative serum from 80 stomach cancer patients, 10 patients bearing benign stomach disease, and 20 matched controls. Glycomic analysis of the total and immunoaffinity depleted serum revealed statistically significant increases in the levels of sialyl Lewis X epitopes (SLe^X) present on triantennary glycans accompanied by increased levels of core fucosylated agalactosyl biantennary glycans present on IgG (referred to as the IgG G0 glycoform) which are associated with increasing disease pathogenesis. Protein expression analysis using 2D-DiGE returned a number of differentially expressed protein candidates in the depleted serum, many of which were shown to carry triantennary SLe^X during subsequent glycomic investigations. Biological pathway analysis of the experimental data returned complement activation and acute phase response signaling as the most significantly altered pathways in the stomach cancer patient serum. Upon the basis of these findings, it is suggested that increased expression of IgG G0 and complement activation are a host response to the presence of the stomach tumor while the increased expression of SLe^X and acute phase response proteins is a result of pro-inflammatory cytokine signaling, including IL-6, during carcinogenesis. The approach presented herein provides an insight into the underlying mechanisms of disease and the resulting changes in the glycome and glycoproteome offer promise as potential markers for diagnosis and prognostic monitoring in stomach cancer.

KEYWORDS: stomach cancer, glycomics, glycoproteomics, 2D-DiGE, pathway analysis, two-dimensional electrophoresis, SLe^X , glycan analysis



INTRODUCTION

Although recent years have witnessed a decline in incidences of cancer of the stomach in the Western World, a diagnosis of stomach adenocarcinoma still carries a poor prognosis due to the lack of specific symptoms, diagnosis being made often only when the cancer has progressed to a late stage and a poor 5 year survival rate of less than 15%.^{1–4} Stomach cancer has an associated complex etiology with many factors thought to contribute to the development and progression of the disease. Sex, age, race,⁵ and

dietary factors, in particular a high salt intake along with the use of nitrate for food preservation are thought to promote the development of cancer of the stomach.⁶ In addition to these environmental factors, *Helicobacter pylori*, a bacterium which is thought to be present in the stomach of half the global population, has also been implicated in the development of gastritis and stomach

Received: October 14, 2010

Published: December 13, 2010

adenocarcinoma.⁷ *H. pylori* is thought to attach to stomach epithelial cells via the interaction of fucosylated and sialylated Lewis type glycan epitopes present on the bacterial cell lipopolysaccharide with Adherin molecules present on the host cell surface.^{8–11} Once attached, *H. pylori* repeatedly delivers the virulent cytotoxin associated gene A protein (CagA) into the stomach epithelial cells where it then undergoes phosphorylation by Src and Abl kinases that confer orthogonal properties to CagA allowing it to interact with and deregulate SHP-2. SHP-2 is a phosphatase which is involved in the regulation of signaling pathways, and also activates NF- κ B which induces the production of pro-inflammatory cytokines.¹² In addition, *H. pylori* infection can cause alterations in the gastric mucosa resulting in atrophy of the mucosal barrier which may increase the risk of carcinogenesis in the underlying epithelial layer.¹³

As early diagnosis remains the key to a more favorable outcome for stomach carcinoma, a considerable research effort has been invested into the discovery of biomarkers for detection of cancerous lesions in the stomach at the early developmental stage of the tumor. While endoscopy remains the gold standard for diagnosis of stomach cancer, the procedure is uncomfortable for the patients and not without risk of complication. Furthermore, patients who do not display symptoms warranting further investigation are generally not selected for endoscopic investigation.^{3,14} The current clinical biomarker, carbohydrate antigen 19-9 (CA19-9), lacks the levels of sensitivity and specificity required to make it clinically useful for the early detection of stomach carcinoma and, as a consequence, has been employed for post resection monitoring rather than diagnostic purposes.^{15–18} In an attempt to discover more suitable and clinically useful biomarker candidates, a number of studies have been reported in the literature wherein genomic^{19–21} and proteomic investigations have been performed using a variety of biological matrices in an attempt to discover alterations in gene or protein expression which offer increased diagnostic potential or provide complementary information to CA19-9. The majority of reported proteomic investigations have been performed using either cancerous tissue or serum due to the relative ease at which such material can be collected. However, studies focusing upon alterations in the saliva proteome²² and the proteome of gastric juice have also been reported in which a general increase in protein concentration was observed along with higher levels of α 1-antitrypsin.^{23,24} Cell culture and mouse xenograft models have also been investigated in order to gain an insight into gastric cancer carcinogenesis^{25–28} and as a source of potential markers wherein decreased levels of apolipoprotein AI²⁹ and increased levels of inter α -tryptsin inhibitor heavy chain H3 (ITIH3)³⁰ were reported in the serum of MNK45 xenograft mice. A number of potential diagnostic and prognostic biomarker candidates have also been reported in the serum of gastric cancer patients using SELDI-Tof-MS for the identification of differentially expressed spectral features,^{31–33} antibody microarrays,³⁴ immunohistochemistry,³⁵ ELISA analysis of target proteins^{36–38}, or two-dimensional electrophoresis (2-DE) with mass spectrometric identification of differentially expressed protein spot features.^{39,40} Of all these reported studies, that of Oue et al.³⁶ who reported the ability of serum olfactomedin 4, a secreted N-linked glycoprotein, to successfully discern patients bearing early stage stomach cancer from healthy individuals as well as those patients bearing more developed tumors with significantly higher sensitivity than CA19-9 is particularly noteworthy. Proteomic comparisons of tumoral tissue versus adjacent nontumoral mucosa has also been

performed in an attempt to discover cancer associated alterations in the proteome that may offer promise as diagnostic or prognostic markers using either immunohistochemical analysis of protein targets suspected to play a role in carcinogenesis and tumor development,^{41–45} direct tissue imaging mass spectrometry of samples collected during resective intervention or endoscopy,^{46,47} or two-dimensional electrophoresis (2-DE) with mass spectrometric identification of differentially expressed protein spot features.^{48–53} However, despite the considerable effort invested in these proteomic studies, none of the reported biomarker candidates have made the transition from the point of discovery to clinical utility.

To date very few reports have been published concerning alterations in the glycome of patients bearing stomach cancer. Of those articles present in the literature, the majority have focused upon the role of carbohydrate epitopes and their involvement in the interaction and binding of *H. pylori* with stomach epithelial cells.^{7–11} Other studies have noted the presence of cancer associated glycan epitopes, for example, the sialyl-Tn antigen, displayed on mucins present in the gastric mucosa⁵⁴ or have studied glycosyltransferase enzymes involved in the biosynthesis of larger branched oligosaccharide structures in the cancerous state and identified proteins present in cancerous and noncancerous gastric tissue displaying such glycans.^{55,56} Few investigations have studied alterations in the glycosylation present on serum proteins in stomach cancer. Goodarzi and Turner⁵⁷ characterized the N-glycosylation present on haptoglobin, selected as a model glycoprotein, to demonstrate alterations in the oligosaccharides present in various disease states including gastric cancer and eluded to the application of the technique for the analysis of potentially clinically useful glycosylation changes in patient samples. More recently, the application of serum glycomics analysis for the discovery of potential glycan based biomarkers in plasma and serum has attracted increased attention. Saldova et al. characterized glycosylation changes present on acute phase proteins and IgG in the serum of ovarian cancer patients in order to gain an insight into the role of glycosylation in disease pathogenesis.⁵⁸ Adb Hamid et al. applied a similar approach for the characterization of alterations in the N-glycosylation present in patients bearing breast cancer and demonstrated in a longitudinal study the ability of the identified glycosylation changes to detect the occurrence of a metastatic event earlier than the current marker, CA15-3.⁵⁹ In a similar study, Pierce et al. reported the ability of similar glycosylation changes to differentiate between lymph node positive and lymph node negative breast cancer.⁶⁰ Alley et al. reported an increased level of α 2–6 linked sialylation present on the glycans of serum glycoproteins of breast cancer patients which is thought to increase the metastatic potential of tumor cells.^{61,62} Kyselova et al. also characterized glycosylation changes in breast cancer serum and noted that increases in sialylation and fucosylation appeared to be indicative of cancer progression.⁶³

In the present study, an investigation into alterations in the serum N-glycome is reported where an increase in the levels of sialyl Lewis X (SLe^X) epitopes on triantennary trisialylated glycans was detected, quantified, and compared to the levels of CA19-9 in the serum of 80 preoperative stomach cancer patients, 10 patients bearing benign stomach disease, and 20 cancer-free matched controls. Accompanying this, an increase in the expression of IgG molecules carrying core fucosylated biantennary agalactosyl glycans was also observed with increasing pathological grade. Using a glycoproteomic approach, serum proteins

displaying the discovered altered oligosaccharide were identified. The levels of SLe^X epitopes on triantennary trisialylated glycans present on each protein isoform, as separated by 2-DE, were evaluated for clinical utility as possible markers for the diagnosis or progression monitoring of stomach cancer. As the identified glycosylation changes were previously reported in studies focusing on other cancers, depletion of the abundant serum proteins was performed in order to try and unearth more cancer specific changes in the serum glycome. Differential protein expression was also investigated using two-dimensional difference in-gel electrophoresis (2D-DiGE). Changes in the depleted stomach cancer glycome were found to be carried by many of the identified differentially expressed protein candidates. To decipher the role of the identified altered glycosylation and protein expression in the pathogenesis of stomach cancer, a bioinformatics investigation using gene ontology and pathway analysis was performed. This suggested that the alterations in the expression of the differentially expressed acute phase proteins carrying SLe^X epitopes on triantennary trisialylated glycans is as a result of increased interleukin-6 (IL-6) signaling while the increased expression of core fucosylated biantennary agalactosyl glycans on IgG molecules in conjunction with the observed increased expression of proteins involved in activation of the complement system suggest a host-defense response to the presence of the stomach tumor.

MATERIALS AND METHODS

Sample Collection

Samples used in this study were provided by RNTech (Bucharest, Romania). Eighty sera samples from preoperative stomach cancer patients, 10 sera samples from patients with benign stomach disease, and 20 sera samples from cancer-free matched controls were collected at the Clinical Institute Fundeni (Bucharest, Romania) from patients with informed consent. Blood samples (5 mL) were drawn into a Vacutte serum tube (Catalogue number 456005, Greiner Bio One, Kremsmuenster, Austria), transferred on ice to the RNTech laboratory, and allowed to clot for approximately 30 min. The tube was then centrifuged at 3000 rpm using a Hettich EBA 20S centrifuge (Hettich Ag, Tuttlingen, Germany) for 5 min at room temperature. The separated serum was subdivided into 1 mL aliquots in sterile cryogenic tubes (Nalgene, Rochester, NY) and immediately frozen at -80 °C. Serum samples were transported on dry ice and stored immediately at -80 °C upon arrival. Each serum sample underwent no more than three freeze/thaw cycles prior to analysis. Details of the clinical parameters on the patients included in the study are provided in Table 1.

N-Glycan Release and Profiling

N-Glycans were released from serum samples using the method of Royle et al.⁶⁴ Briefly, 5 μL of serum was reduced and alkylated via subsequent incubation with dithiothreitol (DTT) and iodoacetamide (IAA) and immobilized in polyacrylamide gel blocks. The gel blocks were transferred to a Whatman Protein Precipitation FF 96 well plate (Lennox Laboratory Supplies, Dublin, Ireland), and washed sequentially with 20 mM sodium hydrogen carbonate buffer, pH 7.0 and acetonitrile. *N*-Glycans were enzymatically liberated via overnight incubation with protein *N*-glycosidase F (PNGaseF, Prozyme, Hayward, CA) at 37 °C. The extracted *N*-glycan pool was then fluorescently labeled with 2-aminobenzamide (Sigma, Dublin, Ireland) via reductive amination for 2 h at 65 °C. Excess fluorophore was

Table 1. Clinical Characteristics of the Patient Serum As Supplied by RNTech

characteristic	number of patients (%)
<i>General Classification</i>	
Noncancer	20
Stomach Benign Disease	10
Stomach Cancer	80
<i>Cancer Type</i>	
Adenocarcinoma	80 (100%)
<i>Age in Years (median, range)</i>	
Noncancer	67.5, 56.4–75.8
Stomach Benign Disease	61.6, 24.3–74.3
Stomach Cancer	65.5, 45.5–77.0
<i>Patient Sex</i>	
Male	77 (70%)
Female	33 (30%)
<i>Pathological Stage (AJCC)^a</i>	
I-b	18 (22.5%)
II	25 (31.3%)
III-a	16 (20%)
III-b	7 (8.8%)
IV	13 (16.3%)
Unknown	1 (1.3%)
<i>Primary Treatment</i>	
Surgical resection	100%
Chemotherapy	0%

^aAJCC, American Joint Committee on Cancer staging system (6th edition).

removed by micro scale paper chromatography using 1 cm² pieces of Whatman 3MM chromatography paper placed in a Whatman Protein Precipitation FF 96 well plate with acetonitrile as the mobile phase. The cleaned *N*-glycan pool was then eluted via subsequent washing of the paper support five times with 200 μL of water. The individual elutions were combined and reduced to dryness in a vacuum centrifuge. The labeled glycans were analyzed by hydrophilic interaction liquid chromatography with fluorescence detection (HILIC-fluorescence) using a TSKgel Amide-80 column, 150 × 4.6 mm, 3 μm particles (Apex Scientific, Kildare, Ireland) using a linear gradient of 35–47% 50 mM ammonium formate pH 4.4 in 48 min. All chromatographic analysis were performed using a Waters Alliance 2695 Separations module with a Waters 2475 Fluorescence Detector under the control of Waters Empower Chromatography Workstation software (Waters, Milford, MA). Retention times were converted to glucose unit (GU) values via time based normalization against a dextran ladder standard. Structural annotation of the resulting chromatographic peaks was performed using a combination of exoglycosidase digestion as previously outlined by Royle et al.⁶⁴ and comparison of retention time data expressed as GU values with GlycoBase.⁶⁵ *N*-Glycan nomenclature used throughout this manuscript was previously described by Harvey et al.⁶⁶

CA19-9 and C-Reactive Protein ELISA

Levels of CA19-9 and C-reactive protein were experimentally determined in the sera of each patient using commercial ELISA kits according to the manufacturer's instructions (BioCheck, Inc., Foster City, CA, part numbers BC-1017 and BC-1119, respectively).

Serum IgG Extraction

Serum IgG antibodies were extracted from each patient sample using Pierce MelonGel spin plates according to the manufacturer's protocol (Medical Supply Company, Dublin, Ireland) and the quantity of extracted protein was determined using the Pierce BCA Protein Assay Kit (Medical Supply Company, Dublin, Ireland). The extracted IgG was then concentrated via vacuum centrifugation, immobilized in a polyacrylamide gel block, and subjected to N-glycan release and HILIC-fluorescence profiling as described above.

Immunoaffinity Depletion of Serum Samples

A subset of serum samples was chosen based upon their pathology and subjected to immunoaffinity depletion of abundant serum proteins using the Agilent Technologies Multiple Affinity Removal Human-14 system (MARS 14, Agilent Technologies, Wilmington, DE, Part No. 5188-6558). The selected samples were randomized prior to depletion in order to prevent the introduction of a processing bias in to the resulting data. A total of 40 μ L of serum was diluted 1:4 using MARS buffer A and centrifuged through a 0.22 μ m spin filter for 1 min at 16 000g to remove particulate material and lipids. The filtrate was then injected onto a 100 \times 4.6 mm i.d. MARS 14 chromatography column using the gradient conditions as described in the manufacturer's instruction manual. The flow through fraction which comprised of serum depleted of the 14 most abundant proteins, albumin, IgG, antitrypsin, IgA, transferrin, haptoglobin, fibrinogen, alpha2-macroglobulin, alpha1-acid glycoprotein, IgM, apolipoprotein AI, apolipoprotein AI, complement C3, and transthyretin, was collected and immediately stored at -80 °C until the time of analysis. The depleted serum fraction was then concentrated via the addition of a 4 \times volume of ice-cold acetone with subsequent overnight incubation at -20 °C followed by centrifugation at 3000g for 30 min. Following centrifugation, the supernatant was discarded, the protein pellet was briefly air-dried and then resuspended in DiGE specific lysis buffer (9.5 M urea, 2% (w/v) CHAPS, 20 mM Tris, pH 8.5). The resuspended pellet was further cleaned using the Ettan 2-D Clean-Up Kit (GE Healthcare, Uppsala, Sweden, catalogue number 80-6484-51) with final resuspension in DiGE specific lysis buffer. The protein concentration was determined using the Bradford assay with BSA standards prepared in DiGE specific lysis buffer in order to avoid any matrix interference effects.

CyDye Reconstitution and Protein Labeling

CyDyes were obtained from GE Healthcare (Uppsala, Sweden) and reconstituted in anhydrous *N,N*-dimethylformamide (DMF, Sigma 227056) according to the supplied product instructions. Twenty-five micrograms of the depleted serum proteins were labeled with 400 pmol Cy5 (GE Healthcare 25-8008-62) and an internal standard comprising an equal concentration of protein in all analytical samples was labeled with 400 pmol Cy3 (GE Healthcare 25-8008-61) using the minimal labeling procedure. All labeling was performed at 4 °C in the dark for 30 min. Following such time, the labeling reaction was quenched via the addition of 1 μ L of 10 mM lysine (Sigma L5626) with subsequent incubation for a further 10 min at 4 °C in the dark. Upon completion of the quenching reaction, an equal volume of 2 \times dilution buffer (9.5 M urea, 2% (w/v) CHAPS, 2% (w/v) DTT, 1.6% (v/v) Pharmalyte pH 3–10) was added to each tube. The internal standard was added to each analytical sample with further dilution to a total volume of 450 μ L with rehydration buffer (8 M urea, 0.5% (w/v) CHAPS, 0.2% (w/v)

DTT, 0.2% (v/v) Pharmalyte) prior to first-dimension isoelectric focusing.

Two-Dimensional Electrophoresis (2-DE) and Two-Dimensional Difference In-Gel Electrophoresis (2D-DiGE)

Both normal 2-DE and 2D-DiGE samples underwent passive overnight in-gel rehydration on 24 cm Immobiline DryStrips pH 3–7 NL for crude serum analysis and pH 4–7 for depleted serum analysis (GE Healthcare, Uppsala, Sweden). Rehydrated strips were then focused using an Ettan IPGphor 3 IEF system. Upon completion of isoelectric focusing, each strip was equilibrated in a reducing equilibration buffer (6 M urea, 50 mM Tris-HCl, pH 8.8, 30% (v/v) glycerol, 2% (w/v) SDS, 1% (w/v) DTT) for 15 min at room temperature followed by subsequent equilibration in an alkylating equilibration buffer (6 M urea, 50 mM Tris-HCl, pH 8.8, 30% (v/v) glycerol, 2% (w/v) SDS, 2.5% (w/v) IAA) for 15 min at room temperature. The IEF strips were then placed on top of 1 mm 12% SDS-PAGE gels and sealed with an agarose sealing solution (192 mM glycine, 25 mM Tris, 0.1% (w/v) SDS, 0.5% (w/v) agarose, 0.02% (w/v) bromophenol blue). Second-dimension SDS-PAGE separation (192 mM glycine, 25 mM Tris, 0.1% (w/v) SDS) was performed in a Bio Rad Protean Plus Dodeca Cell electrophoresis tank (Alpha Technologies, Wicklow, Ireland) using a constant electrophoretic separation power of 1 W/gel overnight at 4 °C. Following completion of the second-dimension separation, gels were either stained using Coomassie Brilliant Blue (0.025% (w/v) in 50% (v/v) methanol, 10% (v/v) glacial acetic acid, 40% (v/v) water) or transferred to PVDF membranes for further immunopropbing. 2D-DiGE gels were immediately scanned using a Typhoon 9410 Variable Mode Imager (GE Healthcare). The photomultiplier tube gain voltage was set to ensure that the maximum pixel intensity for all gel images was within the range of 50 000–65 000 in accordance with the suggestions of Karp et al.^{67,68}

Anti-SLe^X Western Blotting

2-DE gels for immuno probing were immediately transferred upon completion of the electrophoretic run to PVDF membranes using a Multiphor II system (GE Healthcare, Uppsala, Sweden) operating with a constant current of 400 mA for 2 h. To ensure successful protein transfer, the membranes were stained with Ponceau S solution (Sigma P7170) to visualize protein spots and the stain was subsequently removed through repeated washing with Tris Buffered Saline with Tween-20 (TBS-T, 10 mM Tris-HCl, pH 7.5, 100 mM NaCl, 0.2% (v/v) Tween-20). The membranes were blocked overnight at 4 °C in TBS-T containing 5% (w/v) bovine serum albumin (BSA), and following blocking, the membranes were washed in TBS-T (5 times for 5 min). Membranes were then incubated with the anti-SLe^X mouse monoclonal KM93 primary antibody (Calbiochem, Japan, catalogue number S65953, lot number D00076708) which was diluted 1:50 in TBS-T containing 1% (w/v) BSA for 2 h at room temperature with gentle agitation. After such time, the membrane was washed as previously noted with TBS-T and subsequently incubated with the secondary antibody solution for 1 h at room temperature which was horseradish peroxidase linked polyclonal goat anti-mouse IgG (Dako, Glostrup, Denmark) prepared at a 1:1000 dilution in TBS-T containing 1% (w/v) BSA. The membranes were washed extensively as previously described. SuperSignal West Pico chemiluminescent substrate (Pierce, NY) was applied to the membranes for 10 min before development in the dark.

Image Analysis

2D-DiGE Gel images scanned at $100\text{ }\mu\text{m}$ resolution on the Typhoon 9410 Variable Mode Imager were cropped to an appropriate field of interest using ImageQuant version 5.0 (GE Healthcare) and exported into Progenesis SameSpots version 4.0 image analysis software (Nonlinear Dynamics, Newcastle upon Tyne, United Kingdom). The advanced features of Progenesis SameSpots were recently discussed by Kang et al.⁶⁹ Gel images were aligned and automatic analysis was performed on the aligned images using the stepwise wizard functionality within Progenesis SameSpots. The aligned images were grouped according to patient pathology and the returned statistically ranked spot list was evaluated using the data review stage of the software resulting in 41 significant spots for excision and protein identification.

Protein Identification Using LC–MS/MS

Preparative scale gels were run using identical 2-DE conditions as outlined previously. For crude serum experiments, the total protein load per strip was 1 mg, whereas for depleted serum experiments the protein load per strip was 500 μg . Gels were immediately transferred into Coomassie Brilliant Blue stain and stained for 4 h with mild agitation. Excess Coomassie was removed via destaining in 5% (v/v) methanol, 7% (v/v) glacial acetic acid, 88% (v/v) water until minimal background staining was present. Spots of interest were manually excised, washed extensively, and incubated with PNGaseF as previously described in order to liberate any N-glycan material present and thereby facilitate glycosylation profiling via HILIC-fluorescence. Following elution of the N-glycans, the gel pieces were washed further with subsequent applications of acetonitrile and 50 mM ammonium bicarbonate buffer. Protease digestion was performed via overnight incubation with Promega sequencing grade modified trypsin (Medical Supply Company, Dublin, Ireland). The resulting peptides were eluted from the gel pieces via stepwise washing with an increasing concentration of acetonitrile.

LC–MS/MS analysis was performed using an Agilent Technologies 1200 series nano scale HPLC instrument connected via an online nanospray interface to an Agilent Technologies 6340 series ion trap mass spectrometer operated in positive ion mode with a spray voltage of -2.2 kV (Agilent Technologies, Waldbronn, Germany). Tryptic peptides were reconstituted in 0.1% (v/v) aqueous formic acid and loaded onto an Agilent Technologies Zorbax 300SB-C₁₈, 300 $\mu\text{m} \times 5\text{ mm}$, 5 μm enrichment column using a loading flow provided by a 1200 series capillary pump at $20\text{ }\mu\text{L min}^{-1}$ and separated using a linear gradient of acetonitrile on an Agilent Technologies Zorbax 300 SB-C₁₈, 0.075 \times 150 mm, 3.5 μm column at a flow rate of 300 nL min^{-1} . All data was acquired with the mass spectrometer operating in automatic data dependent switching mode using a MS/MS fragmentation amplitude of 1.4. A maximum resolution scan was performed on the two most intense ions in order to determine charge state prior to MS/MS analysis.

Data from MS/MS experiments was analyzed using Agilent Technologies Spectrum Mill Proteomics Workbench version A.03.03.084 SR4 (Agilent Technologies, Santa Clara, CA). The MS/MS data was searched against the National Centre for Biotechnology Information database using the human mouse taxonomic filter. The following search parameters were used: precursor ion mass tolerance of 2.5 Da, product ion mass tolerance of 0.7 Da with cysteine carbamidomethylation specified as a fixed modification and asparagine deamidation and methionine oxidation specified as variable modifications and a maximum

of two missed cleavage sites allowed. Returned protein identifications were automatically validated using the autovalidation feature of Spectrum Mill, peptide scores >6 , protein scores >11 and the percentage scored peak intensity $>60\%$. In addition to this, spectra were also manually inspected and verified.

Bioinformatics

Proteins which were found to be differentially expressed were compared to all annotated proteins by functional grouping based upon gene ontology (GO) annotation using the Web based DAVID program.⁷⁰ The differentially expressed proteins were also analyzed using Ingenuity Pathway Analysis (IPA, version 8.6) and GeneGO Metacore pathway analysis software (version 4.3) in an attempt to discover significantly altered biological processes or pathways. Pathways returned with P -values ≤ 0.001 were considered as significant.

Statistical Analysis

Statistical analysis of all glycomic data was performed using SPSS statistical analysis software Version 15.0 for Windows (Dublin, Ireland); tests used included Kruskall–Wallis and Mann–Whitney nonparametric tests. In all instances, a P -value <0.05 was considered as being statistically significant. Multivariate statistical analysis of HILIC-fluorescence data was performed using Umetrics Simca-P+ software version 11.5 (Umetrics, Ascot, United Kingdom).

RESULTS

Alterations in the Serum N-Glycome in Stomach Cancer

To investigate the presence of cancer related alterations in the serum glycome, the discovery phase glycomics analysis was performed using two complementary methods, (1) HILIC-fluorescence profiling of the total serum N-glycan pool with multivariate statistical analysis (principal component analysis, PCA, and partial least-squares differential analysis, PLS-DA) of the resulting chromatographic data and (2) off-line two-dimensional liquid chromatographic separation and analysis of pathologically staged pooled released N-glycans. Profiling was performed in triplicate using a fresh serum aliquot from the patient replicates as provided by RNTech. In each instance, 20 distinct chromatographic peaks were integrated as illustrated in Figure 1A. The average relative percentage peak area for each peak from the three resulting patient replicate analyses was used for subsequent multivariate statistical analysis of the resulting chromatographic data.

PCA and PLS-DA variable importance (VIP) plots generated using multivariate statistical analysis of the averaged global glycosylation HILIC-fluorescence profiles for the stomach cancer patients with comparison to the stomach benign disease and the reduced noncancer patient cohorts are depicted in Figure 1. The PCA analysis was capable of generating a partial separation of the patient classifications; however, there is still a significant degree of overlap. For the initial PCA analysis as depicted in Figure 1B, a general ‘stomach cancer’ grouping was used. Inclusion of the TNM classification data as provided by RNTech in the accompanying patient clinical data did not improve the multivariate model. This suggests that a refinement of the data is necessary to discover which glycosylation features display the most relevance in aiding classification of patients based upon disease status. The PLS-DA VIP analysis as depicted in Figure 1C aids in a limited way to discover such features by ranking the chromatographic peaks in order of contribution to the PCA

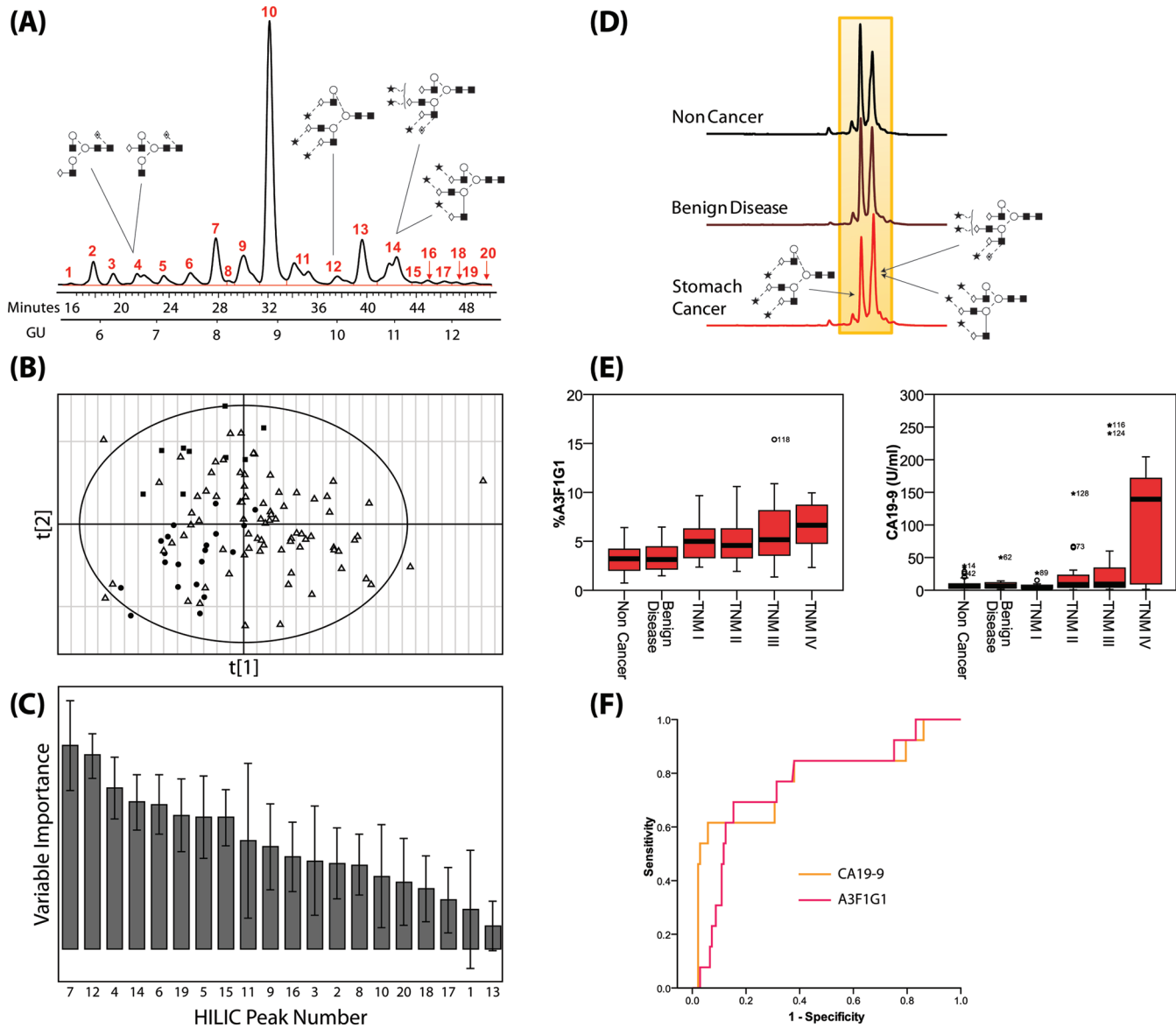


Figure 1. Discovery of alterations in the stomach cancer serum N-glycome, (A) representative HILIC-fluorescence chromatogram displaying the 20 distinct and integrated peaks as used for multivariate statistical analysis along with the glycan structures present in the peaks returned as being the most statistically significant; for details regarding the glycan symbolic representation see ref 66. (B) Principle component analysis (PCA) scatter plot generated using the broad classification of noncancer (●), stomach benign disease (■), and stomach cancer (△) HILIC-fluorescence glycan profiles. (C) Partial least-squares differential analysis variable importance plot (PLS-DA VIP) displaying the HILIC-fluorescence peaks in order of significance based upon their contribution to the PCA scatter plot in panel B. (D) HILIC-fluorescence chromatograms of the trisialylated fraction as separated by anion exchange chromatography displaying the alteration in the relative proportions of the peak on the left which contains triantennary glycans carrying α2-3/6-linked sialic acids in favor of the peak on the right which contains triantennary glycans carrying α2-6-linked sialic acids and trisialylated triantennary glycans carrying a sialyl Lewis X epitope (SLe^X). (E) Box plots of the levels of the SLe^X digestion product, A3F1G1 and CA19-9, plotted against TNM stage as the grouping variable displaying an increase in A3F1G1 and CA19-9 with disease progression. (F) Receiver operator characteristic (ROC) curve as generated in SPSS to evaluate the performance of the A3F1G1 SLe^X digestion product as a possible biomarker versus CA19-9.

separation. From Figure 1C it can be seen that highest ranked peaks were peak 4 which contains biantennary asialo monogalactosylated glycans typically found in the Fc region of IgG antibody molecules, and peak 12 which contains triantennary glycans carrying α2-3-linked sialic acids, and peak 14 which contains triantennary glycans carrying α2-6-linked sialic acids and trisialylated triantennary glycans carrying a sialyl Lewis X epitope (SLe^X). The statistical significance of these changes was further investigated using nonparametric statistical tests. It was found that there was a statistically significant decrease in the relative

percentage areas of peak 4 and peak 12 with TNM stage as the grouping variable (Kruskal-Wallace analysis, $P = 8.83 \times 10^{-5}$ at the 95% confidence level for peak 4 and $P = 3.35 \times 10^{-4}$ at the 95% confidence level for peak 12) and a statistically significant increase in the relative percentage area of peak 14 with TNM stage as the grouping variable (Kruskal-Wallace analysis, $P = 2.19 \times 10^{-5}$ at the 95% confidence level for peak 14).

To improve the chromatographic separation and hence the feature number for comparison, off-line two-dimensional liquid chromatography was employed wherein the glycans were

separated by charge, that is, their degree of sialylation, in the first dimension on a weak anion exchange stationary phase followed by profiling each of the collected charge separated fractions using HILIC-fluorescence. The resulting data was aligned and normalized to facilitate identification of possible alterations in the levels of the glycans present. Figure 1D displays the HILIC-fluorescence trace of the trisialylated glycan fraction from each of the patient classes. This fraction contained the most notable differences of all the charge fractions. From Figure 1D it can be seen that the ratio of the two major peaks present is altered in the cancerous state as compared to that present in the noncancerous state. Exoglycosidase digestion and comparison of the digestion data with GlycoBase revealed that the peak on the left contains triantennary trisialylated glycans carrying a mixture of $\alpha 2-3$ and $\alpha 2-6$ -linked sialic acids while the peak on the right which increases in the cancerous state is a mixture of two species, a triantennary trisialylated glycan carrying only $\alpha 2-6$ -linked sialic acids but also a triantennary trisialylated glycan carrying a SLe^X epitope. Similar observations were also recently reported in the serum N-glycan pool from patients bearing breast^{59,62} and ovarian cancers.⁵⁸

Quantitation of the levels of the SLe^X epitope present on the triantennary glycan by selectively digesting the released N-glycans with sialidase (*Arthrobacter ureafaciens*) and $\beta 1-4$ galactosidase (*Streptococcus pneumoniae*) was then performed. Each of the triplicate glycan pools from each individual patient was digested with the exoglycosidase enzymes with subsequent profiling of the digestion products by HILIC-fluorescence. Sialidase (*A. ureafaciens*) and $\beta 1-4$ galactosidase (*S. pneumoniae*) selectively digest the triantennary trisialylated glycan carrying the SLe^X epitope to a structure denoted A3F1G1, a triantennary monogalactosylated glycan carrying an alpha linked fucose residue on one of the antennary N-acetyl glucosamine residues. The peak corresponding to the digestion product A3F1G1 was quantified based upon the relative percentage peak area of this structure in the resulting HILIC-fluorescence chromatograms and the average of the triplicate measurement was then statistically analyzed via Kruskal-Wallis analysis in SPSS, version 15.0. To compare the clinical utility of the A3F1G1 digestion product of the SLe^X epitope to that of the current protein marker CA19-9, the levels of CA19-9 were experimentally determined using a commercially available ELISA. The analysis was performed in triplicate. The average of the three replicate measurements was also analyzed via Kruskal-Wallis analysis in SPSS, version 15.0. Both the levels of A3F1G1 and CA19-9 were found to show a statistically significant increase versus TNM stage as the grouping variable (Kruskal-Wallis analysis, $P = 1.78 \times 10^{-6}$ at the 95% confidence level for the relative percentage area of A3F1G1 and $P = 2.37 \times 10^{-4}$ at the 95% confidence level the concentration of CA19-9, Figure 1E displays the resulting box plots). The Spearman's nonparametric test was performed to investigate a possible correlation between the levels of A3F1G1 and CA19-9; however, no correlation between the variables was returned (Spearman $\rho = 0.056$, $R^2 = 0.156$).

To examine the performance of the identified glycosylation change further, Receiver-Operator Characteristic (ROC) curves were generated from the experimental CA19-9 and A3F1G1 data using SPSS version 15.0 as depicted in Figure 1F. The area under the curve (AUC) values were determined as 0.779 and 0.758 for CA19-9 and A3F1G1, respectively, thereby suggesting similar performance of both CA19-9 and A3F1G1 as potential diagnostic or prognostic markers. AUC values of 0.7–0.8 are considered

moderately accurate.⁶² Upon the basis of the experimentally determined AUC values, individually, CA19-9 and A3F1G1 do not offer the levels of clinical sensitivity and specificity required for accurate diagnosis of stomach cancer. However, due to the similarity in performance, the combination of A3F1G1 with CA19-9 when used in its current prognostic role may help increase the confidence of the clinical measurement.

Alterations in the Glycosylation of Serum IgG Show an Increase in Agalactosyl Glycoforms with Cancer Progression

Two of the most significant HILIC-fluorescence peaks (peaks 4 and 7) as returned by the PLS-DA analysis corresponded to biantennary glycans similar to those known to be present on the Fc domain of IgG molecules.⁷¹ To probe these observations further, IgG was extracted from the provided serum samples in triplicate. The concentration of the enriched IgG was determined and N-glycans were liberated and profiled using HILIC-fluorescence as outlined above. Malhotra et al. previously described pro-inflammatory properties of the agalactosyl G0 glycoform of IgG due to its potential to act as a ligand for mannose binding lectin with subsequent complement activation.⁷² The ratio of agalactosyl to monogalactosyl (G0/G1) N-glycans of serum IgG in each of the patient sera samples was determined to examine the behavior of the G0/G1 ratio in the cancerous state. Levels of C-reactive protein (CRP), a commonly used inflammation marker, were also experimentally determined using a commercially available ELISA. Statistical analysis of the experimental data using the Kruskal-Wallis nonparametric test in SPSS, version 15.0, revealed a statistically significant increase in the G0/G1 ratio, $P = 1.48 \times 10^{-10}$ at the 95% confidence level using TNM stage as the grouping variable. No statistical significance was present in the concentrations of IgG and CRP as determined. The data indicates that in the cancerous state there is a switch in IgG production toward the more pro-inflammatory IgG G0 glycoform. A proposed reason for such an alteration in glycosylation may reflect a host defense mechanism directed against the tumor cell, wherein specific clones of B-cells are activated to produce IgG G0 antibodies against an antigen on the tumor cell surface. The exposed G0 glycan in the Fc domain of the IgG molecule may then be recognized by mannose binding lectin followed by complement activation leading potentially to tumor cell lysis.

Identification of Serum Proteins Carrying the Identified Glycosylation Changes and Evaluation of Clinical Utility

Having identified alterations in the serum glycome of the stomach cancer patients, the question as to the identity of the serum proteins carrying the glycans in question was then posed as these glycoproteins may offer more promise as potential markers rather than the individual glycans. The approach undertaken in order to identify proteins carrying SLe^X involved a mixture of two-dimensional electrophoresis (2-DE) and anti-SLe^X Western blotting followed by LC-MS/MS identification of the highlighted protein features. Master patient classification pools of sera were prepared during the course of the glycomics analysis by taking a 5 μ L aliquot of serum from each patient. These master pools were used for initial glycoproteomic investigations. In addition to this, TNM staged pools were also prepared based upon the clinical data as provided by RNTech for each of the cancer patients. These TNM staged pools were used for the evaluation of the diagnostic or prognostic opportunity of the altered glycosylation present on individual protein isoforms as detected in the initial investigations. The protein concentration

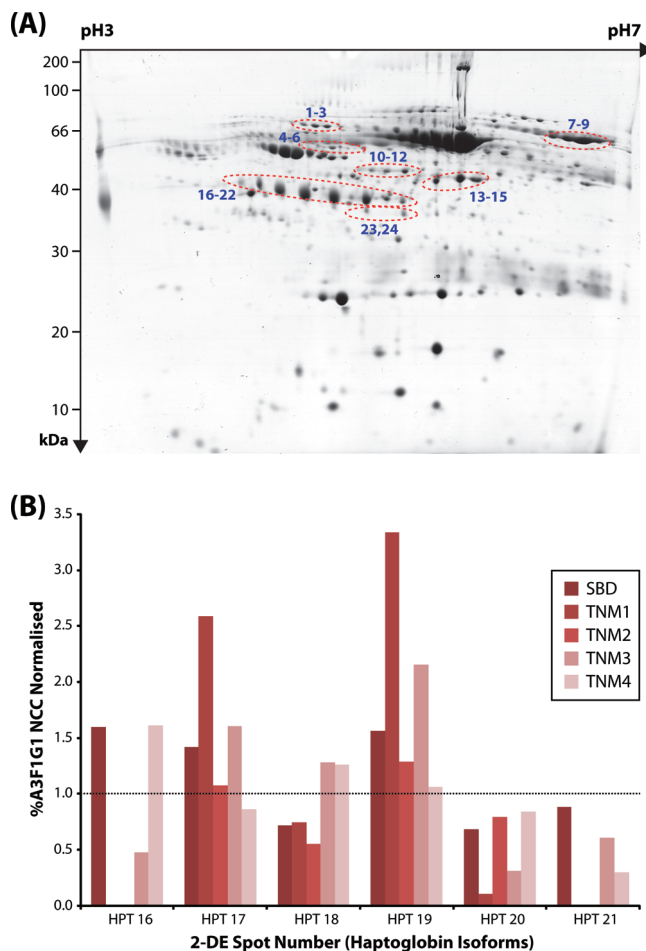


Figure 2. (A) Representative Coomassie stained 2-DE separation of stomach cancer serum, IEF pH range 3–7 NL in the first dimension followed by 12% PAGE in the second; the highlighted proteins were those as identified by the anti-SLe^X Western blot using the KM 93 antibody. (B) Quantification of the levels triantennary SLe^X present on individual isoforms of haptoglobin β-chain excised from pathologically staged 2-DE gels and normalized to the levels of A3F1G1 as determined on the noncancer patient gels. Insufficient glycan material was present on spot HPT22 to permit quantitation.

of each of these master and disease staged sera pools was determined using the BCA protein assay. In each instance, the serum volume corresponding to 1 mg of total protein was used for 2-DE analysis.

Figure 2A is a representative Coomassie stained 2-DE gel image for the master stomach cancer serum pool along with Table 2 which lists the identification of the protein spot features as highlighted by the anti-SLe^X Western blot. N-glycans were also released from the excised gel plugs prior to protease digestion in order to cross validate the anti-SLe^X Western blot and to also identify the spot features that carried triantennary glycans displaying SLe^X epitopes as identified previously. Of the proteins identified, only haptoglobin β-chain was found to contain SLe^X present on triantennary glycans in sufficient quantities in order to permit further evaluation.

The 2-DE spot features corresponding to haptoglobin β-chain were then excised from the TNM staged 2-DE gels. N-glycans were liberated and digested with sialidase (*A. ureafaciens*) and

β1–4 galactosidase (*S. pneumoniae*) and profiled via HILIC-fluorescence in order to permit quantitation of the triantennary SLe^X digestion product A3F1G1. The resulting relative percentage area data for A3F1G1 was normalized as fold change relative to the quantities of A3F1G1 present in the noncancer patient cohort spots and plotted as a bar graph as depicted in Figure 2B. 2-DE gels per individual pathological classification were run in triplicate but the excised spots were combined in order to maximize material, as a consequence a caveat of the data presented in Figure 2B represents the digestion of the released glycan pool and a single HILIC-fluorescence analysis.

It can be seen from Figure 2B that there appears to be a general but modest rise in the levels of SLe^X present on the more acidic haptoglobin β-chain spots in the diseased state, both benign and cancerous, when normalized against the levels of SLe^X present for the noncancerous state. However, levels of SLe^X present in spot HPT 17 and spot HPT 19 on the TNM I patient pool were 2.5- and 3.5-fold higher, respectively, as compared to the noncancer cohort and the patients with benign disease. Although preliminary in nature and it is noted that further validation would be required in order to clearly establish any possible degree of clinical utility, the data suggests that the levels of SLe^X present on these two particular haptoglobin β-chain isoforms may offer promise for the early detection of stomach cancer.

Glycomic Profiling of Depleted Serum to Improve Cancer Specificity

A subset of the provided sera samples was selected based upon their pathology as outlined in the clinical data as supplied by RNTEch. Seven of the noncancer patient cohort, the 10 provided stomach benign disease patients, 8 stomach cancer patients with early stage cancer as described by their TNM score (2b,1,0, Level II), and 8 stomach cancer patients with metastatic cancer as described by their TNM score (2b,1,1 Level IV) were chosen and subjected to immunoaffinity base serum depletion as previously described. In an analogous manner to the crude serum, the N-glycans present on the depleted serum proteins were released and profiled by both HILIC-fluorescence and off-line two-dimensional liquid chromatography. The average of the three replicate measurements from each patient was determined and then subjected to multivariate statistical analysis using Umetrics Simca P+, version 11.5. A number of different data combinations were examined including the ability of the depleted glycan profiles to separate noncancer and benign disease from each of the cancers. However, the most interesting PCA based separations were recorded when investigating the ability of the depleted glycan profiles to differentiate between the early and metastatic staged stomach cancer patients as depicted in Figure 3A.

Excellent clustering of the patients present in each cohort was observed in the PCA plots (Figure 3A) based upon the combination of the chromatographic peaks present in the HILIC-fluorescence chromatograms. Upon further inspection of the data, it was observed that a patient from each class seemed to be misclassified in the resulting PCA plot. When the clinical information was checked further, it was noted that the information provided was contradictory for the patient belonging to the TNM (2b,1,1 Level IV) cohort while it appears that the two early stage stomach cancer patients falling outside the clustering ellipse had larger tumor volumes than the other patients of same TNM level present inside the clustering ellipse.

Off-line two-dimensional liquid chromatography was also performed using patient N-glycan pools prepared according to

Table 2. Proteomic Identification Data for the 2-DE Separated Stomach Cancer Crude Serum Protein Spot Features As Highlighted by the Anti-SLe^X Western Blot^a

spot no.	protein(s) identified by LC-MS/MS	UniProt accession number	summed MS/MS search score	no. of distinct peptides	% sequence coverage
1	Alpha-1 β -glycoprotein	P04217	65.49	5	13
2	Alpha-1 β -glycoprotein	P04217	95.04	7	17
3	Alpha-1 β -glycoprotein	P04217	153.76	10	32
4	Vitamin D Binding Protein	P02774	185.41	12	39
	α -1-antitrypsin	P01009	50.24	3	10
	Antithrombin	P01008	30.22	6	2
	Angiotensin	P01019	37.58	2	5
5	Vitamin D Binding Protein	P02774	279.52	17	49
6	Vitamin D Binding Protein	P02774	121.84	9	28
	Antithrombin	P01008	64.37	4	14
7	Transferrin	P02787	446.31	27	46
	IGHM	P01871	51.78	4	10
8	Transferrin	P02787	484.98	30	49
9	Transferrin	P02787	416.49	26	46
	IGHM	P01871	40.96	3	7
10	Albumin	P02768	114.39	10	21
11	Albumin	P02768	269.69	17	38
12	Albumin	P02768	274.88	18	35
13	Albumin	P02768	272.98	16	25
	Haptoglobin	P00738	53.82	4	9
14	Albumin	P02768	236.73	14	24
15	Albumin	P02768	201.73	12	20
16	Haptoglobin	P00738	76.63	6	12
17	Haptoglobin	P00738	172.53	11	28
18	Haptoglobin	P00738	130.12	8	22
19	Haptoglobin	P00738	134.00	8	21
20	Haptoglobin	P00738	176.78	11	26
21	Haptoglobin	P00738	167.05	10	24
22	Haptoglobin	P00738	143.80	9	28
23	Haptoglobin	P00738	124.43	8	20
24	Haptoglobin	P00738	94.09	7	17

^a The spot numbers as listed correspond to those inserted on the gel image presented in Figure 2A.

their pathological classification. After HILIC-fluorescence profiling of the anion exchange fractionated sample pools, the data was aligned and normalized to facilitate identification of possible alterations in the levels of the glycans present as per Figure 3B. A number of changes in the glycosylation were noted. In the neutral fraction, an increase in the peak at GU 6.2 (Man5GlcNAc2) was observed only in the TNM level IV patient cohort. In addition, levels of tetraantennary tetrasialylated glycans present which increased with disease progression are consistent with reports describing an increase in branching and sialylation in cancer.^{63,73}

The most interesting change in glycosylation of the low-abundance proteins noted in the stomach cancer patients was present in the trisialylated fraction in an analogous manner as observed during the total serum glycomics analysis. Here the ratio of the peak containing the trisialylated triantennary glycan to the peak containing the trisialylated triantennary glycan carrying a SLe^X epitope and the trisialylated triantennary carrying only α 2–6-linked sialic acids remained constant in the non-cancer and benign disease patient cohorts, was almost equal in the stomach cancer TNM II patient cohort, and finally shifted in favor of the peak containing the trisialylated triantennary glycan

carrying a SLe^X epitope and the trisialylated triantennary carrying only α 2–6-linked sialic acids in the stomach cancer TNM IV patient cohort. This was in contrast to the crude serum analysis where the shift toward the peak containing the trisialylated triantennary glycan carrying a SLe^X epitope and the trisialylated triantennary carrying only α 2–6-linked sialic acids was present in all but the noncancer patient cohort, thereby suggesting an increased degree of cancer specificity.

To further investigate these observations, the depleted serum glycans of each patient were digested with sialidase (*A. ureafaciens*) and β 1–4 galactosidase (*S. pneumoniae*) and profiled via HILIC-fluorescence to permit quantitation of the SLe^X digestion product A3F1G1. No statistical significance was returned using the Kruskal–Wallace analysis of the levels of A3F1G1 present in all the patient cohorts versus TNM stage as the grouping variable. Each possible individual combination of patients was also tested for statistical significance using the Mann–Whitney test. Of these combinations, the levels of A3F1G1 present between the noncancer patient cohort and the stomach cancer TNM IV patient cohort was returned as being statistically significant, $P = 0.040$ at the 95% confidence level.

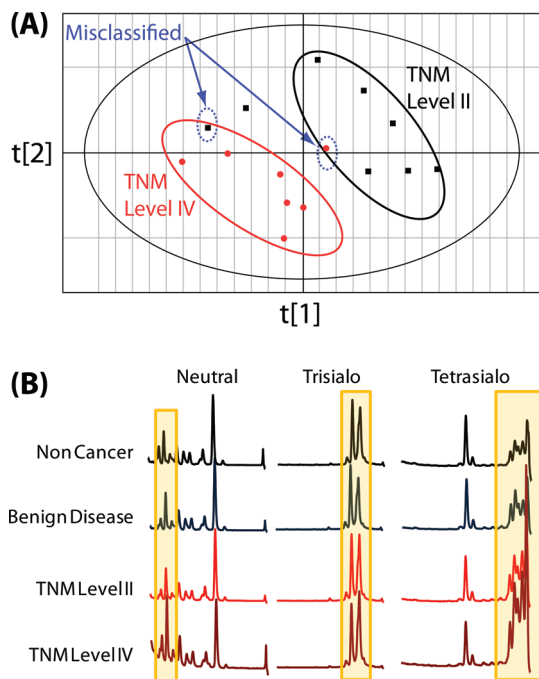


Figure 3. (A) PCA scatter plot generated using the HILIC-fluorescence depleted serum N-glycan profiles of stomach TNM Level II versus the TNM Level IV patients. (B) HILIC-fluorescence chromatograms of the neutral, tri-, and tetrasialylated fractions of the depleted serum N-glycome as separated by anion exchange chromatography displaying alterations in the levels of glycans present. In the neutral fraction, the increased peak in the TNM Level IV trace corresponds to an increase in Man₅GlcNAc₂, and the alteration in the trisialylated fraction is as previously described in Figure 1 D. For the depleted serum, the change was gradual with disease progression, and in the tetrasialylated fraction, a general increase in all structures was observed with disease progression.

Differential Proteomic and Glycoproteomic Analysis of the Depleted Serum To Identify Differentially Expressed Cancer Associated Protein Targets and Proteins Carrying the Identified Altered Glycosylation

Protein expression analysis within the depleted serum proteins was performed using 2D-DiGE, first dimension pH 4–7. All possible patient combinations were considered and analyzed during image analysis using Progenesis SameSpots and returned protein spot features displaying significant changes, that is, P values ≤ 0.05 and fold changes >1.5 were selected and excised from preparative scale Coomassie Brilliant Blue stained 2-DE gels (500 μ g protein load) run under identical experimental conditions for identification, Figure 4A. A complete PCA based separation of patient classes was observed in most instances for each of the possible combinations posed within Progenesis SameSpots. However, when comparing the TNM Level II patient group versus the TNM Level IV group, it was not possible to separate these patient cohorts based upon the proteomic data. Conversely, the glycomics data was able to separate the two distinct cancer stages based upon their depleted serum N-glycan profiles. In total, 41 spot features were returned from all the clinical scenarios posed within Progenesis SameSpots as highlighted in Figure 4A, and of these, all but two were successfully identified by LC–MS/MS analysis as listed in Table 3. In the majority of cases, a single protein was identified per spot; however, seven spots were identified to contain two or more proteins. All identifications were performed with a minimum of two distinct peptides.

Proteins that were observed to be differentially expressed were then checked for functional relevance using a number of bioinformatic tools. The DAVID⁷⁰ Web resource was used to determine the molecular function of the candidate list based upon their gene ontology. Processes returned were defense response and immune response in the presence of wounding or inflammation, homeostasis and protein processing, complement activation, B-cell mediated immunity, and lipid transport and metabolism. The number of proteins assigned to a particular function was high most probably attributable to the high degree of multifunctionality of many serum proteins. The list of differentially expressed proteins was also analyzed using Ingenuity Pathway Analysis (IPA, version 8.6) in an attempt to discover significantly altered biological processes or pathways. The top two canonical pathways identified as being significantly enriched within the experimental data set were 'acute phase response signaling', $P = 7.89 \times 10^{-18}$ and 'Complement system', $P = 2.44 \times 10^{-7}$. Figure 5 displays a simplified version of each of the returned canonical pathways.

Glycoproteomic investigations were also performed to see if any of the differentially expressed proteins or indeed other low-abundance serum proteins were carrying any of the previously identified glycosylation changes, in particular trisialylated triantennary glycans carrying a SLe^X epitope. N-Glycans from the protein features excised from the preparative scale gels were profiled via HILIC-fluorescence both undigested and digested with sialidase (*A. ureafaciens*) and β 1–4 galactosidase (*S. pneumoniae*) in order to permit more confident detection of trisialylated triantennary glycans carrying a SLe^X epitope by monitoring the presence of its digestion product, A3F1G1. In addition, a 2-DE anti-SLe^X Western blot was also performed and any additional protein spot features highlighted were excised, deglycosylated to permit N-glycan profiling, and subsequently protease digested with trypsin in order to facilitate protein identification via LC–MS/MS. Table 4 lists the identification data of these additionally highlighted protein spot features.

In total, 10 proteins were identified as carriers of the trisialylated triantennary glycans carrying a SLe^X epitope in the depleted serum glycoproteome by both HILIC-fluorescence profiling and the anti-SLe^X Western blot. To evaluate the clinical utility of these observed glycosylation changes, pooled pathologically staged patient cohort gels were run. The released N-glycans from the highlighted protein spot features were digested with sialidase (*A. ureafaciens*) and β 1–4 galactosidase (*S. pneumoniae*) to permit quantitation of A3F1G1 via HILIC-fluorescence profiling. The resulting data was normalized against the quantity of A3F1G1 present on the spots excised from the noncancer patient gels and is presented in Figure 4B. As was previously mentioned when performing such an analysis using the crude serum 2-DE spots, these experiments were only performed singly due to the amount of patient material required to generate such data and therefore serve as trend indicators. Further validation of the data is required prior to any further clinical application. Most notably, the levels of SLe^X present on leucine rich- α 2-glycoprotein, haptoglobin, and kininogen-1 were observed to increase with relevance to TNM score, while the levels of SLe^X present on clusterin were observed to decrease in line with TNM score, Figure 4 B.

The other noted change in the stomach cancer glycome was an increase in the levels of Man₅ in the stomach TNM IV depleted serum glycome. To identify which depleted serum proteins were potentially displaying the Man₅GlcNAc₂ structure, 100 μ g of

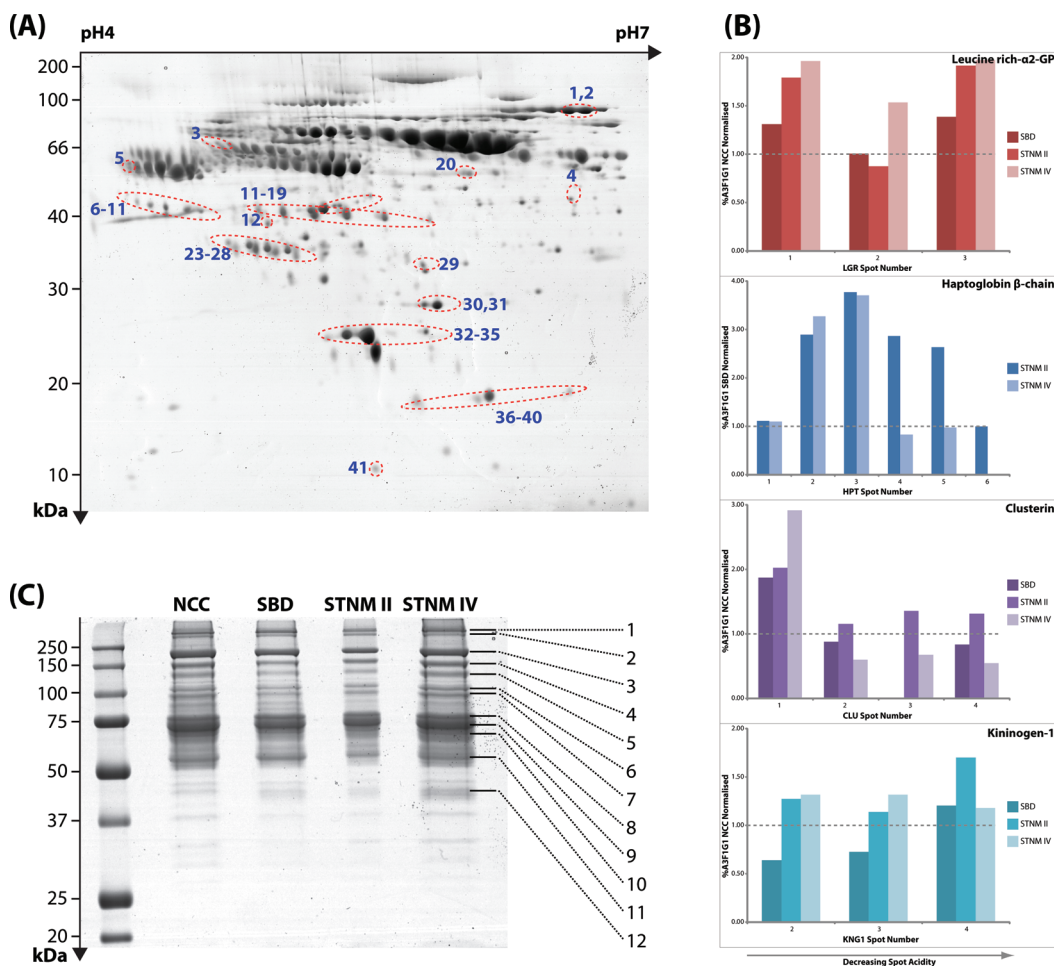


Figure 4. (A) Representative 2-DE separation of depleted stomach cancer serum, IEF pH range 4–7 in the first dimension followed by 12% PAGE in the second; the highlighted proteins were those identified as being differentially expressed by 2D-DiGE, and the spot numbers correspond to those as listed in Table 3. (B) Quantification of the levels of triantennary SLe^X present on individual isoforms of leucine rich- α 2-acid glycoprotein, haptoglobin β -chain, clusterin, and kininogen-1 excised from pathologically staged 2-DE depleted serum gels and normalized to the levels of A3F1G1 as determined on the noncancer patient gels with the exception of haptoglobin β -chain wherein the data is normalized to the levels present on the stomach benign disease patient gels as no haptoglobin β -chain was presented on the noncancer cohort gels after serum depletion. (C) One dimensional 10% reducing SDS-PAGE separation of the glycoproteins present in the depleted serum as enriched using the Pierce ConA glycoprotein kit. The numbers of the bands correspond to those listed in Table 5 which contains the LC-MS/MS protein identification data.

protein from each of the pathologically significant depleted serum pools was extracted using the Concavallin A glycoprotein isolation kit (Pierce) according to the manufacturer's instructions. An equal concentration of enriched protein was then separated by one-dimensional reducing SDS-PAGE, and the resulting gel was stained with Coomassie Brilliant Blue, Figure 4C. Bands were excised, deglycosylated, and tryptically digested and analyzed via LC-MS/MS to identify the proteins present. The resulting proteomic identification data is presented in Table 5.

DISCUSSION

Glycans as biomarkers or indicators that may provide an insight into the molecular mechanisms of disease pathogenesis is an area of research that has attracted increased interest in recent years.^{74–76} Serum remains the biofluid of choice for the discovery of such glycan based biomarkers due to the relative ease at which it can be collected and also due to the fact that serum, by virtue of the intimate contact of the blood with tissues, both normal and malignant, is likely to contain proteins and

glycoproteins shed by tumoral tissue which are detected as alterations in the levels of target analytes then present in the serum.⁷⁷ Furthermore, as protein glycosylation is known to become altered during malignant transformation, altered levels of oligosaccharides present on serum glycoproteins in disease represent an exciting area that offers the potential of a new source of biomarkers.^{78,79} Here, an investigation into alterations in the serum glycome of patients with stomach cancer revealed an increase in the levels of triantennary trisialylated N-glycans carrying α 2–6-linked sialic acids and also triantennary trisialylated N-glycans carrying a SLe^X epitope. Glycoproteomics was performed to discover which serum proteins were displaying the altered glycan structures. To identify more specific cancer changes in the serum glycome, abundant protein depletion was performed using the Agilent Technologies MARS14 depletion system. Identified changes in the depleted serum glycome, proteome, and glycoproteome were evaluated for clinical utility and subjected to bioinformatics analysis using gene ontology and pathway analysis. This suggested that the alterations in the expression of the differentially expressed acute phase proteins carrying

Table 3. Proteomic Identification Data for Protein Spot Features Returned as Being Differentially Expressed by 2D-DiGE^a

spot no.	protein(s) identified by LC-MS/MS	UniProt accession number	summed MS/MS search score	no. of distinct peptides	% sequence coverage	SLe ^X detected on glycans
1	Complement factor B	P00751	202.83	13	23	Yes
2	Complement factor B	P00751	243.42	15	26	-
3	Kininogen-1	P01042	106.22	7	15	Yes
4	Complement Factor H	P08603	26.04	2	4	-
5	Serpin peptidase inhibitor, Clade A Vitronectin	P01011 P04004	54.20 32.32	4 2	12 8	Yes
6	Leucine rich alpha-2-glycoprotein	P02750	28.14	2	9	Yes
7	Leucine rich alpha-2-glycoprotein	P02750	65.16	4	20	Yes
8	Leucine rich alpha-2-glycoprotein	P02750	69.33	5	21	Yes
9	C4A Variant protein Coagulation factor II precursor variant	P0COL4 P00734	62.12 40.39	4 3	4 7	Yes
10	Leucine rich alpha-2-glycoprotein	P02750	45.93	3	14	Yes
11	Haptoglobin	P00738	65.17	4	10	Yes
12	Zn-alpha2-glycoprotein	P25311	42.16	3	13	Yes
13	Haptoglobin	P00738	100.95	7	16	Yes
14	Haptoglobin Apolipoprotein A-IV Precursor	P00738 P06727	48.94 47.43	4 3	9 10	Yes
15	Haptoglobin Apolipoprotein A-IV Precursor	P00738 P06727	43.21 66.14	3 4	8 13	Yes
16	Haptoglobin	P00738	92.95	6	13	Yes
17	Haptoglobin Apolipoprotein A-IV Precursor	P00738 P06727	77.71 27.72	5 2	12 5	Yes
18	Haptoglobin	P00738	99.14	6	16	Yes
19	Haptoglobin	P00738	84.95	5	11	Yes
20	Galectin 7 Tubulin alpha 2 or alpha 6 SFN Stratifin S100 Calcium binding protein A9	P47929 Q13748 P31947 P06702	54.92 46.90 46.20 40.45	3 3 3 3	30 8 19 35	-
21	Haptoglobin	P00738	39.81	2	5	-
22	UNIDENTIFIED	-	-	-	-	-
23	Clusterin isoform 1	P10909	51.70	3	8	Yes
24	Clusterin isoform 1	P10909	60.37	4	10	Yes
25	Clusterin isoform 1	P10909	40.12	3	7	Yes
26	Clusterin isoform 1	P10909	120.15	7	13	Yes
27	Clusterin isoform 1	P10909	70.11	5	13	Yes
28	Clusterin isoform 1	P10909	69.82	4	8	-
29	Inter alpha trypsin inhibitor family HCIP	P19827	25.01	2	3	-
30	Serum amyloid P component precursor	P02743	110.45	8	39	-
31	Serum amyloid P component precursor	P02743	151.02	10	33	-
32	Apolipoprotein A-I Preproprotein	P02647	94.91	6	29	-
33	Apolipoprotein A-I Preproprotein	P02647	149.90	9	34	-
34	Apolipoprotein A-I Preproprotein	P02647	39.12	5	9	-
35	Apolipoprotein A-I Preproprotein	P02647	34.32	2	10	-
36	Haptoglobin isoform	P00738	26.12	3	6	-
37	Haptoglobin isoform	P00738	15.89	3	6	-
38	Haptoglobin isoform	P00738	60.22	4	11	-
39	Haptoglobin isoform	P00738	30.72	2	7	-
40	UNIDENTIFIED	-	-	-	-	-
41	Transthyretin	P02766	55.87	2	17	-

^a The spot numbers as listed correspond to those inserted on the gel image presented in Figure 4A.

SLe^X epitopes on triantennary trisialylated glycans result from increased pro-inflammatory cytokine production, such as IL-6

signaling. Increased expression of core fucosylated biantennary agalactosyl glycans on IgG molecules in conjunction with

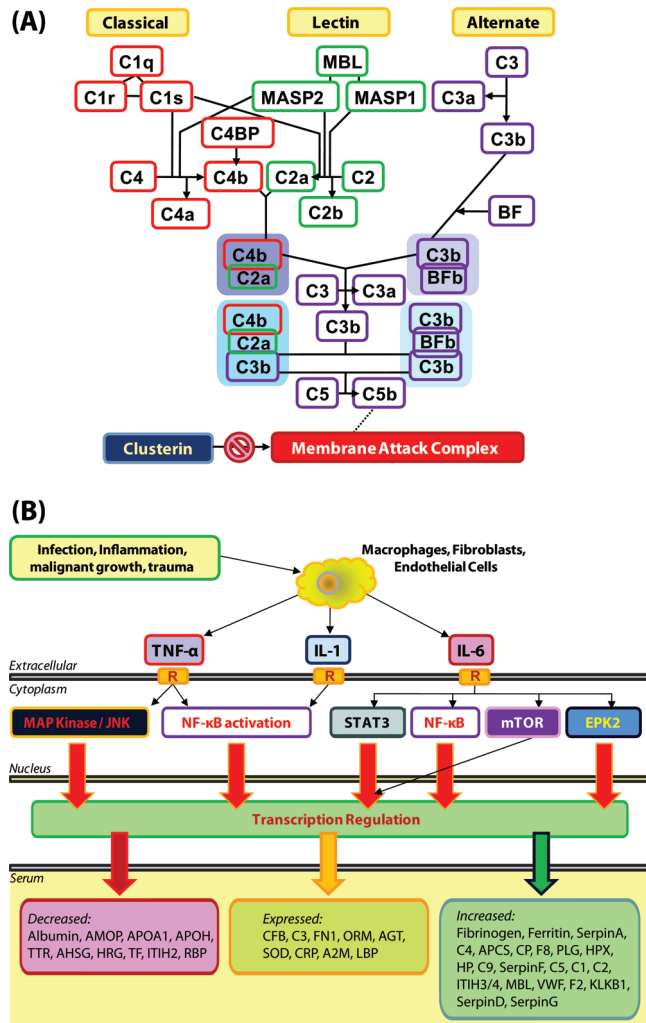


Figure 5. Overrepresented biological pathways as identified by IPA and GeneGo. (A) Up-regulation of complement activation and down-regulation of clusterin in conjunction with increased expression of IgG carrying core fucosylated G0 type glycans as identified during the serum glycomics analysis suggesting a host defense response to the presence of the stomach carcinoma. (B) Up-regulation of the acute phase response due to the increased production of pro-inflammatory cytokines such as IL-6.

observed increased expression of proteins involved in activation of the complement system suggest a host-defense response to the presence of the stomach tumor.

Identification of Cancer Associated Alterations in the Serum Glycome of Stomach Cancer Patients

The glycomics analysis of the total serum N-glycome revealed two major changes in the glycans present. First, an increase in the chromatographic peak containing triantennary trisialylated N-glycans carrying α 2–6-linked sialic acids and triantennary trisialylated N-glycans carrying a SLe^X epitope correlated with disease progression. The increase in α 2–6-linked sialic acids on serum glycoproteins has also recently been reported by Alley et al. who noted similar changes in breast cancer patients.⁶² The increased expression of glycans terminating in α 2–6-linked sialic acid has been previously reported with poor prognosis in many human cancers.⁸⁰ Gretsche et al. described the use of a radiometric assay to monitor the activity of the ST6GAL-I and ST3GAL-III

sialyltransferase enzymes in gastric cancer tissues and nontumoral mucosa samples and reported an enhancement in the levels of ST6GAL-I activity within the tumor tissue.⁵⁶ This increased expression of ST6GAL-I did not independently influence the prognosis of gastric tumors; the most important parameter relating to a poor prognostic outcome was lymph node metastasis.⁵⁶ Despite this observation, other reports have shown that the increased expression of α 2–6-linked sialic acids on tumor cell surface glycoproteins can affect the functions of β -integrin resulting in a significantly higher affinity for collagen-I and laminin present in the extracellular matrix with accompanied increased haptotactic migration toward collagen-I, thereby suggesting increased motility and extravasation of cancerous cells and more facilitated cancer progression.⁸¹

Increased levels of the SLe^X epitope present on triantennary trisialylated N-glycans observed in the current study has been reported in other human cancers.^{58,59} SLe^X is a tetrasaccharide which is synthesized *in vivo* by the activity of the α 2–3 sialyltransferases ST3GAL and the α 1–3 fucosyltransferases FUT3, FUT5, FUT6, and FUT7.⁸² Of these glycosyltransferases, reports indicate that FUT7 plays a dominant role in SLe^X biosynthesis.^{83,84} Ikeguchi et al.⁸⁵ previously reported increased levels of the pro-inflammatory cytokine IL-6 in the serum of patients with stomach cancer. Both IL-6 and tumor necrosis factor- α (TNF- α) increase the expression of glycosyltransferases involved in SLe^X biosynthesis in bronchial mucosa.^{86,87} These observations provide a rationale for the increased levels of the triantennary trisialylated N-glycans carrying a SLe^X epitope with increasing disease progression. SLe^X structures are recognized by selectin molecules present on the surfaces of platelets, endothelia, and innate immune cells.^{80,88} The processing of SLe^X epitopes on tumor cell surface glycoproteins may represent an evolutionary accomplishment by the tumor cell to exploit the interaction of SLe^X with selectins for transport, after extravasation, through the vasculature to a secondary site for the propagation of metastases.^{80,88} Such an effect was previously outlined by Ono and Hakamori⁸⁹ who described higher metastatic potential of colorectal cancer cells displaying SLe^X. Furthermore Amado et al. reported positive correlation of high levels of SLe^X expression with venous invasion and poor overall prognosis in a study of 97 gastric carcinomas.⁹⁰ In addition to this, Koike et al.⁹¹ described the effect of hypoxic conditions which are likely to be a more accurate reflection of the anaerobic environment in developing tumors and demonstrated increased expression of SLe^X and SLe^A on the surface of colon cancer cells which resulted in increased cancer cell adhesion to endothelial E-selectin. The hypoxic conditions resulted in increased transcription of the genes encoding FUT7 and ST3GAL-I, glycosyltransferases involved in SLe^X biosynthesis, and also in genes for syndecan-4 and α 5-integrin, cell adhesion molecules involved in the adhesion of cancer cells to fibronectin.⁹¹ Therefore, it was demonstrated that the increased expression of SLe^X on the cancer cell surface resulted in an enhancement in binding to vascular endothelial cells via both selectin and integrin mediated pathways and led to an increased metastatic potential of the cancer.⁹¹ These literature reports corroborate with the experimental findings in this study wherein increased levels of SLe^X in the total serum N-glycome correlated with disease progression. From these observations, it therefore appears that levels of SLe^X are a good marker for monitoring the prognostic potential and also provide complementary information to the current marker CA19-9, as illustrated by the experimentally determined areas under the ROC curve

Table 4. Proteomic Identification Data for the Additional 2-DE Separated Depleted Stomach Cancer Serum Protein Spot Features As Highlighted by the Anti-SLe^X Western Blot

spot no.	protein(s) identified by LC-MS/MS	UniProt accession number	summed MS/MS search score	no. of distinct peptides	% sequence coverage
1	Serpin peptidase inhibitor, Clade A	P01011	84.40	5	16
2	Serpin peptidase inhibitor, Clade A	P01011	143.19	9	30
	Kininogen-1	P01042	29.46	2	3
3	Serpin peptidase inhibitor, Clade A	P01011	166.40	10	26
	Kininogen-1	P01042	84.62	7	11
4	Serpin peptidase inhibitor, Clade A	P01011	179.21	12	33
	Kininogen-1	P01042	89.00	7	15
5	Serpin peptidase inhibitor, Clade A	P01011	172.76	11	31
	Kininogen-1	P01042	128.24	10	17
6	Serpin peptidase inhibitor, Clade A	P01011	61.10	4	14
7	Serpin peptidase inhibitor, Clade A	P01011	73.94	5	18
8	Serpin peptidase inhibitor, Clade A	P01011	66.67	4	14
	α 2-HS-glycoprotein	P02765	36.27	2	9
	Kininogen-1	P01042	24.37	2	4
9	Serpin peptidase inhibitor, Clade A	P01011	71.03	4	15
	Kininogen-1	P01042	57.08	4	8
	α 2-HS-glycoprotein	P02765	36.93	2	9
10	Serpin peptidase inhibitor, Clade A	P01011	89.31	6	18
	Kininogen-1	P01042	45.23	3	7
	α 2-HS-glycoprotein	P02765	37.94	2	9
11	Kininogen-1	P01042	36.53	3	5
	α 2-HS-glycoprotein	P02765	33.76	2	9

Table 5. Proteomic Identification Data for the 1-D SDS-PAGE Gel Bands Present in Figure 4C after Enrichment of the Depleted Stomach Cancer Serum Using the Pierce ConA Glycoprotein Enrichment Kit in an Attempt to Identify Which Depleted Serum Proteins Were Displaying Elevated Levels of ManSGlcNAc2

band no.	protein(s) identified by LC-MS/MS	UniProt accession number	summed MS/MS search score	no. of distinct peptides	% sequence coverage
1	Interalpha-trypsin inhibitor heavy chain H2	P19823	42.79	3	4
2	Interalpha-trypsin inhibitor heavy chain H2	P19823	47.65	3	4
3	Complement Factor H	P08603	41.65	3	3
4	Ceruloplasmin	P00450	60.38	4	5
5	Interalpha-trypsin inhibitor HCRP	Q14624	47.35	3	5
6	Plasma protease C1 inhibitor	P05155	28.10	2	6
7	C4A Variant Protein	P0C0L4	64.88	4	4
	Plasma protease C1 inhibitor	P05155	43.77	3	9
8	α -1 β -glycoprotein	P04217	52.50	4	13
9	Serpin peptidase inhibitor, Clade A	P01011	30.93	2	8
10	Serpin peptidase inhibitor, Clade A	P01011	96.47	7	18
11	Serpin peptidase inhibitor, Clade A	P01011	42.73	3	8
12	Haptoglobin	P00738	36.04	2	4

of 0.779 and 0.758 for CA19-9 and A3F1G1, respectively (Figure 1F).

Increased IgG G0 Accompanied by Up-Regulation of Complement May Suggest a Host Defense Response to the Stomach Carcinoma

The second major change recorded in the serum *N*-glycome was an increase in the levels of core fucosylated biantennary agalactosyl glycans on extracted IgG antibody molecules (IgG G0). The origin of such glycans on IgG molecules may be due to one of two events, either a decrease in galactosyltransferase activity in plasma cells as was previously noted by Axford and

co-workers in autoimmune rheumatoid disease⁹² or the presence of circulating plasma cells with specifically low galactosyltransferase activities.⁹³ It has been previously demonstrated that these particular glycoforms of IgG may illicit a pro-inflammatory response as a result of their ability to act as ligands for mannose binding lectin and subsequent complement activation.^{72,94,95} As was revealed by our 2D-DiGE and subsequent gene ontology and pathway analysis of the differentially expressed proteins, the return of complement activation as a statistically significantly altered pathway in the present study corroborates with the observation of increased expression of IgG carrying core fucosylated

G0 type glycans. Furthermore, the current observation suggests that the expression of IgG carrying core fucosylated G0 type glycans may represent a host response to the presence of the stomach carcinoma. Increased expression of IgG carrying core fucosylated G0 type glycans with specificity against an antigen on the tumor cell surface may result in subsequent complement activation with tumor cell lysis via the membrane attack complex. As also experimentally noted, the increase in the levels of IgG carrying core fucosylated G0 type glycans occurs in association with disease progression. Similar findings by Kanoh et al.⁹⁶ also reported an increase in core fucosylated biantennary agalactosyl glycan expression on serum IgG determined using fluorophore assisted carbohydrate electrophoresis (FACE) and suggested that such an alteration in glycosylation may offer promise as a diagnostic and prognostic marker for patients bearing stomach cancer.

Abundant Protein Depletion Facilitates a Deeper Look into the Serum Glycome for the Discovery of Cancer Associated Glycosylation Changes

As part of the current study, abundant proteins were removed from the serum using the commercially available Agilent Technologies MARS-14 chromatography column in order to search for more cancer specific changes in the glycome, proteome, and glycoproteome. A novel aspect of the data is the glycomics analysis of the depleted serum. As expected, abundant protein depletion resulted in a marked change in the resulting N-glycan profile of the depleted serum, most notably the almost complete disappearance of chromatographic peaks corresponding to core fucosylated asialo-biantennary glycans. However, considering that such structures are predominantly displayed on IgG molecules and MARS-14 depletion removes IgG, the absence of these particular glycans provides an indication as to the success of the depletion procedure. Another interesting point is the remaining presence of bi-, tri-, and tetrasialylated glycans present in the depleted serum N-glycan profile with minimal variation in the resulting peak areas between the total serum N-glycan pool and the depleted serum N-glycan pool. This observation therefore suggests that these glycans are also present in measurable quantities on low-abundance proteins and alterations in the glycosylation present on these proteins may be a source of more cancer specific markers. Similar findings were also recently noted by Bereman and Muddinam who profiled the N-glycans present in serum both before and after MARS-6 depletion.⁹⁷

Serum Haptoglobin Displays Increased Levels of SLe^X with Cancer Progression

Glycoproteomics analysis of the crude serum to identify which proteins are displaying the increased levels of SLe^X was performed using a combination of 2-DE, anti-SLe^X Western blotting, and LC-MS/MS identification of the resulting spots. Of all the highlighted features, only haptoglobin was identified as carrying SLe^X epitopes on triantennary glycans. More interestingly, after abundant protein depletion and 2D-DiGE analysis, haptoglobin was again retuned as a statistically significant differentially expressed protein. For both the crude and depleted serum 2-DE separation of haptoglobin isoforms, subsequent quantitation of the levels of SLe^X present on triantennary glycans revealed significantly higher levels in the cancerous state as opposed to that present in the benign and noncancer patient groups, suggesting that SLe^X present on haptoglobin may offer promise as a marker for diagnosis and prognostic monitoring of stomach cancer. He et al. and Saldova et al. analyzed the

glycosylation present in the 2-DE separated haptoglobin isoforms and reported similar oligosaccharides and also noted that the origin of the haptoglobin spot train present after 2-DE separation occurs due to increased sialylation present in the more acidic spot features.^{98,58} Haptoglobin is a homotetramer consisting of 2α and 2β subunits held together by inter chain disulfide bonds. Increased levels of fucosylation have previously been reported in other human cancers including hepatocellular,⁹⁹ non-small cell lung carcinoma,¹⁰⁰ and proposed as a biomarker for pancreatic cancer.^{101–103} The occurrence of increased fucosylation, both core and antennary fucosylation has been studied by Miyoshi and co-workers.^{104,105} They hypothesized that the increased levels of fucosylated haptoglobin present in pancreatic cancer patient serum was due to two distinct possibilities, either production of fucosylated haptoglobin by pancreatic cancer cells or the production of a factor by pancreatic cancer cells that induces the increased production of fucosylated haptoglobin by the liver.¹⁰² Further studies demonstrated that IL-6 expressed by pancreatic cancer cells stimulated the production of haptoglobin displaying increased fucosylation by Hep3B hepatoma cells.¹⁰⁵ Real-time PCR analysis was used to show that genes encoding fucosyltransferases were all up-regulated following IL-6 treatment.¹⁰⁵ A site specific analysis of haptoglobin present in the serum of patients with pancreatic cancer, chronic pancreatitis, as well as healthy individuals demonstrated an increase in the levels of triantennary N-glycans carrying SLe^X epitopes at Asn211.¹⁰⁴ In the current study, the presence of haptoglobin and its return as a differentially expressed protein spot feature were considered surprising considering that haptoglobin should have been depleted from the serum using the MARS-14 immunodepletion column. It is suggested that the presence of haptoglobin in the MARS-14 depleted serum occurs due to two possibilities, either a dramatic increase in the levels of haptoglobin present in the serum of stomach carcinoma patients or, based upon the knowledge base of Miyoshi et al., cancer induced alterations in glycosylation potentially induces either a conformational change in the tertiary structure of haptoglobin or alternatively masks the antigen recognition site of the antibody used for immunodepletion. As the volume of serum used for each individual depletion was always only 80% of that as recommended by the manufacturer's protocols, it is unlikely that the capacity of the column was exceeded in any one serum injection.

Other differentially expressed proteins returned by 2D-DiGE carrying triantennary SLe^X included clusterin, leucine-rich-α2-glycoprotein, and kininogen-1.

Clusterin Is Down-Regulated in Stomach Cancer Serum and Displays Smaller N-Glycans with Cancer Progression

Clusterin in serum exists as a heterodimer of two nonidentical subunits, each of an approximate molecular mass of 35 kDa. It has been reported that the carbohydrate moiety of clusterin accounts for approximately 30% of the mass of the glycoprotein which contains seven potential N-glycosylation sites.¹⁰⁶ A defined function has yet to be annotated for clusterin. However, it has been demonstrated that clusterin can bind to and inactivate the membranolytic potential of the membrane attack complex of the complement system.¹⁰⁷ Clusterin has also been implicated in cellular functions involved in carcinogenesis and tumor progression.¹⁰⁸ More recently, reports of deregulation of clusterin in cancer have been reported. Andersen et al. compared clusterin mRNA expression between normal mucosa and tumoral tissue in colorectal cancer and noted reduced expression of clusterin

mRNA possibly due to suppression of the stromal compartment in the tumor.¹⁰⁹ Zoubeidi et al. investigated the role of clusterin in the survival of prostate cancer cells and noted that clusterin serves as a ubiquitin-binding protein that enhances COMMD1 and I- κ B proteasomal degradation and thereby increases NF- κ B nuclear translocation and transcriptional activity.¹¹⁰ In the current study, clusterin expression was found to be down-regulated in the serum of stomach cancer patients when compared to patients diagnosed with benign stomach conditions. Furthermore, the glycosylation present on the individual clusterin isoforms was also found to be altered with cancer progression (Figure 4B) wherein a shift from trisialylated triantennary glycans to disialylated biantennary glycans correlated with cancer progression. The purpose of the current study was not to elucidate the role of clusterin in stomach carcinoma patients; however, the experimental data potentially suggest that down-regulation of clusterin with a shift to smaller glycan structures is a host response to the stomach tumor.

Altered Glycosylation Present on Up-Regulated Leucine-rich α 2-Glycoprotein May Be a Cancer Associated Pro-Survival Factor

In this study, leucine rich- α 2-glycoprotein (LRG) was also differentially expressed with increased levels in the serum of stomach cancer patients with disease progression. Increased expression of LRG in the serum of pancreatic cancer patients was reported by Kakisaka et al.¹¹¹ suggesting that the increased expression of LRG with disease progression is cancer associated rather than cancer specific. LRG is a 347 amino acid residue glycoprotein with four N-linked glycosylation sites and one O-linked glycosylation site at threonine 37. Within the amino acid sequence lie eight repeating consensus sequences rich in leucine, proline, and asparagine, the so-called leucine rich repeats that provide a structural motif that facilitates protein–protein interactions.¹¹² Up-regulation of LRG expression is mediated by IL-6 signaling.¹¹² Although the function of LRG in the serum remains undefined, Jemmerson and co-workers demonstrated that LRG binds extracellular cytochrome C and *in vitro* is a survival factor for lymphocytes and other cells that are susceptible to the toxic effects of extracellular cytochrome C.^{113,114} In the current study, increased quantities of LRG were observed in stomach cancer patient serum with increasing carcinogenesis. In addition, increased levels of SLe^X were present on the glycans of LRG with increasing pathogenesis. Glycosylation is known to affect the half-life and clearance of proteins in the serum. A potential explanation is increased expression of LRG by tumor cells or tumor induced increased expression of LRG by the liver in an analogous manner as was reported for haptoglobin.¹⁰⁴ This may indicate that the increased levels of LRG acts as a pro-survival tumor factor by exploiting altered glycosylation to extend their serum half-life and effectively scavenge cytochrome C, thus, preventing apoptotic cell death.

Kininogen-1 Carries High Levels of SLe^X in Both Normal and Cancer Patient Serum

An interesting observation of the current study was very high levels of SLe^X present on triantennary glycans on kininogen-1, up to 25% of the total glycans present. Increased sialylation and fucosylation was previously reported in the plasma of patients with colorectal cancer using lectin glycoarrays.¹¹⁵ However, the data presented herein (Figure 4B) represent the first glycan structural analysis of the oligosaccharides present on kininogen-1. Kininogen-1 and related kinins play a role in vasodilatation,

vascular permeability enhancement and cell migration and pain, and kininogen-1 has recently been demonstrated to bind to macrophages.¹¹⁶ Decreased expression of kininogen-1 was observed with increasing pathogenesis in the current study and accompanied by small fold changes in the levels of SLe^X present on triantennary glycans. Although it was expected that the high levels of SLe^X on kininogen-1 might infer a role in either macrophage recruitment or tumor cell escape via exploitation of the inherent vasodilatation functions of kininogen-1, no such effects can be reported.

Biological Pathway Enrichment Analysis Suggests the Origin of the Observed Changes in the Glycome and Proteome May Be Due to Increased IL-6 Signaling

Biological pathway analysis identified acute phase response signaling as being significantly overexpressed in the current study, Figure 5. Analysis of the literature has indicated that the changes we have observed in both the proteome and glycome of the stomach cancer patients may be associated with increased pro-inflammatory cytokine signaling in the cancerous state. The bank of knowledge generated during this study provides an insight into the molecular mechanisms of stomach carcinoma pathogenesis and may act as potential markers providing complementary information to CA19-9 or indeed provide targets for therapeutic intervention.

CONCLUSION

Alterations in the serum glycome, proteome, and glycoproteome of stomach cancer patients were investigated in an attempt to discover potential biomarkers for early diagnosis or pathogenesis progression monitoring. The levels of triantennary glycans carrying a SLe^X epitope were significantly increased with disease progression as were IgG G0 antibody glycoforms. 2D-DIGE revealed a number of differentially expressed proteins also identified to carry altered glycosylation. Biological pathway analysis of the entire data set suggests that the increased expression of IgG G0 antibody glycoforms in conjunction with over activation of the complement system are host defense reaction responses to the presence of the stomach tumor. In following with other reports in the literature, the increased expression of SLe^X epitopes along with increased acute phase response signaling are consistent with increased activity of the pro-inflammatory cytokine, IL-6. It is foreseen that with further validation the levels of SLe^X on haptoglobin β -chain and LRG along with the levels of IgG G0 could potentially offer clinical utility as markers for monitoring cancer progression when used in conjunction with other diagnostic tools such as CA19-9 screening.

AUTHOR INFORMATION

Corresponding Author

*Tel: +353 1716 6725. E-mail: pauline.rudd@nibrt.ie.

ACKNOWLEDGMENT

This research was supported by the European Union via the EU FP6 GLYFDIS research program, grant reference 037661. We would like to thank Dr. William E. P. Greenland from Agilent Technologies and Mr. Stefan Mittermayr for their technical assistance. Prof. Irinel Popescu, Prof. Serban Bubeneck Turconi, and Prof. Liliana Livia Paslaru at the Clinical Institute Fundeni and Laura Ciobanu and Michael Bia at

RNTech are also kindly acknowledged for their roles in sample collection and distribution.

■ REFERENCES

- (1) Jemal, A.; Siegel, R.; Ward, E.; Hao, Y.; Xu, J.; Thun, M. J. Cancer statistics, 2009. *CA Cancer J. Clin.* **2009**, *59*, 225–249.
- (2) Allum, W. H. Gastric cancer in Europe. *Br. J. Surg.* **2008**, *95*, 406–408.
- (3) Maconi, G.; Manes, G.; Porro, G. B. Role of symptoms in diagnosis and outcome of gastric cancer. *World J. Gastroenterol.* **2008**, *14*, 1149–1155.
- (4) Cancer research UK, Stomach cancer—key facts, available online via <http://info.cancerresearchuk.org/cancerstats/types/stomach/index.htm?script=true>, last accessed Jul 31, 2010.
- (5) Yamaoka, M.; Nakajima, S. Prevalence of subjects at a high or very high risk of gastric cancer in Japan. *Gut Liver* **2009**, *3*, 95–100.
- (6) Saikawa, Y.; Fukuda, K.; Takahashi, T.; Nakamura, R.; Takeuchi, H.; Kitagawa, Y. Gastric carcinogenesis and the cancer stem cell hypothesis. *Gastric Cancer* **2010**, *13*, 11–24.
- (7) Peek, R. M., Jr.; Blaser, M. J. Helicobacter pylori and gastrointestinal tract adenocarcinomas. *Nat. Rev. Cancer* **2002**, *2*, 28–37.
- (8) Kobayashi, M.; Lee, H.; Nakayama, J.; Fukuda, M. Carbohydrate-dependent defense mechanisms against Helicobacter pylori infection. *Curr. Drug Metab.* **2009**, *10*, 29–40.
- (9) Liu, T. W.; Ho, C. W.; Huang, H. H.; Chang, S. M.; Popat, S. D.; Wang, Y. T.; Wu, M. S.; Chen, Y. J.; Lin, C. H. Role for alpha-L-fucosidase in the control of Helicobacter pylori-infected gastric cancer cells. *Proc. Natl. Acad. Sci. U.S.A.* **2009**, *106*, 14581–14586.
- (10) Johansson, L.; Johansson, P.; Miller-Podraza, H. Neu5Acalpha3Gal is part of the Helicobacter pylori binding epitope in poly-glycosylceramides of human erythrocytes. *Eur. J. Biochem.* **1999**, *266*, 559–565.
- (11) Prakobphol, A.; Borén, T.; Ma, W.; Zhixiang, P.; Fisher, S. J. Highly glycosylated human salivary molecules present oligosaccharides that mediate adhesion of leukocytes and Helicobacter pylori. *Biochemistry* **2005**, *44*, 2216–2224.
- (12) Hatakeyama, M. Helicobacter pylori and gastric carcinogenesis. *J. Gastroenterol.* **2009**, *44*, 239–248.
- (13) Jia, Y.; Persson, C.; Hou, L.; Zheng, Z.; Yeager, M.; Lissowska, J.; Chanock, S. J.; Chow, W. H.; Ye, W. A comprehensive analysis of common genetic variation in MUC1, MUC5AC, MUC6 genes and risk of stomach cancer. *Cancer Causes Control* **2010**, *21*, 313–321.
- (14) Choi, J.; Kim, S. G.; Im, J. P.; Kim, J. S.; Jung, H. C.; Song, I. S. Comparison of endoscopic ultrasonography and conventional endoscopy for prediction of depth of tumor invasion in early gastric cancer. *Endoscopy* **2010**, *42* (9), 705–713.
- (15) Carpelan-Holmström, M.; Louhimo, J.; Stenman, U. H.; Alfthan, H.; Haglund, C. CEA, CA 19-9 and CA 72-4 improve the diagnostic accuracy in gastrointestinal cancers. *Anticancer Res.* **2002**, *22*, 2311–2316.
- (16) Carpelan-Holmström, M.; Louhimo, J.; Stenman, U. H.; Alfthan, H.; Järvinen, H.; Haglund, C. CEA, CA 242, CA 19-9, CA 72-4 and hCGbeta in the diagnosis of recurrent colorectal cancer. *Tumor Biol.* **2004**, *25*, 228–234.
- (17) Feldman, A. L.; Espina, V.; Petricoin, E. F., 3rd; Liotta, L. A.; Rosenblatt, K. P. Use of proteomic patterns to screen for gastrointestinal malignancies. *Surgery* **2004**, *135*, 243–247.
- (18) Qiu, M. Z.; Lin, J. Z.; Wang, Z. Q.; Wang, F. H.; Pan, Z. Z.; Luo, H. Y.; Li, Y. H.; Zhou, Z. W.; He, Y. J.; Xu, R. H. Cut off value of carcinoembryonic antigen and carbohydrate antigen 19-9 elevation levels for monitoring recurrence in patients with resectable gastric adenocarcinoma. *Int. J. Biol. Markers* **2009**, *24*, 258–264.
- (19) Chen, Y.; Song, Y.; Wang, Z.; Yue, Z.; Xu, H.; Xing, C.; Liu, Z. Altered expression of MiR-148a and MiR-152 in gastrointestinal cancers and its clinical significance. *J. Gastrointest. Surg.* **2010**, *14*, 1170–1179.
- (20) Wang, Y. Y.; Ye, Z. Y.; Zhao, Z. S.; Tao, H. Q.; Li, S. G. Systems biology approach to identification of biomarkers for metastatic progression in gastric cancer. *J. Cancer Res. Clin. Oncol.* **2010**, *136*, 135–141.
- (21) Gige, C. O.; Leal, M. F.; Silva, P. N.; Lisboa, L. C.; Lima, E. M.; Calcagno, D. Q.; Assumpção, P. P.; Burbano, R. R.; Smith Mde, A. hTERT methylation and expression in gastric cancer. *Biomarkers* **2009**, *14*, 630–636.
- (22) Wu, Z. Z.; Wang, J. G.; Zhang, X. L. Diagnostic model of saliva protein finger print analysis of patients with gastric cancer. *World J. Gastroenterol.* **2009**, *15*, 865–870.
- (23) Lee, K.; Kye, M.; Jang, J. S.; Lee, O. J.; Kim, T.; Lim, D. Proteomic analysis revealed a strong association of a high level of α1-antitrypsin in gastric juice with gastric cancer. *Proteomics* **2004**, *4*, 3343–3352.
- (24) Hsu, P. I.; Chen, C. H.; Hsieh, C. S.; Chang, W. C.; Lai, K. H.; Lo, G. H.; Hsu, P. N.; Tsay, F. W.; Chen, Y. S.; Hsiao, M.; Chen, H. C.; Lu, P. J. α1-antitrypsin precursor in gastric juice is a novel biomarker for gastric cancer and ulcer. *Clin. Cancer Res.* **2007**, *13*, 876–883.
- (25) Takikawa, M.; Akiyama, Y.; Maruyama, K.; Suzuki, A.; Liu, F.; Tai, S.; Ohshita, C.; Kawaguchi, Y.; Bandou, E.; Yonemura, Y.; Yamaguchi, K. Proteomic analysis of a highly metastatic gastric cancer cell line using two-dimensional differential gel electrophoresis. *Oncol. Rep.* **2006**, *16*, 705–711.
- (26) Tomlinson, A. J.; Hincapie, M.; Morris, G. E.; Chicz, R. M. Global proteome analysis of a human gastric carcinoma. *Electrophoresis* **2002**, *23*, 3233–3240.
- (27) Zhang, X. W.; Sheng, Y. P.; Li, Q.; Qin, W.; Lu, Y. W.; Cheng, Y. F.; Liu, B. Y.; Zhang, F. C.; Li, J.; Dimri, G. P.; Guo, W. J. BMI1 and Mel-18 oppositely regulate carcinogenesis and progression of gastric cancer. *Mol. Cancer* **2010**, *9*, 40–51.
- (28) Florou, D.; Papadopoulos, I. N.; Scorilas, A. Molecular analysis and prognostic impact of the novel apoptotic gene BCL2L12 in gastric cancer. *Biochem. Biophys. Res. Commun.* **2010**, *391*, 214–218.
- (29) Chong, P. K.; Lee, H.; Zhou, J.; Liu, S. C.; Loh, M. C.; So, J. B.; Lim, K. H.; Yeoh, K. G.; Lim, Y. P. Reduced plasma APOA1 level is associated with gastric tumor growth in MKN45 mouse xenograft model. *J. Proteomics* **2010**, *73*, 1632–1640.
- (30) Chong, P. K.; Lee, H.; Zhou, J.; Liu, S. C.; Loh, M. C.; Wang, T. T.; Chan, S. P.; Smoot, D. T.; Ashktorab, H.; So, J. B.; Lim, K. H.; Yeoh, K. G.; Lim, Y. P. ITIH3 is a potential biomarker for early detection of gastric cancer. *J. Proteome Res.* **2010**, *9*, 3671–3679.
- (31) Qiu, F. M.; Yu, J. K.; Chen, Y. D.; Jin, Q. F.; Sui, M. H.; Huang, J. Mining novel biomarkers for prognosis of gastric cancer with serum proteomics. *J. Exp. Clin. Cancer Res.* **2009**, *28*, 126–132.
- (32) Poon, T. C.; Sung, J. J.; Chow, S. M.; Ng, E. K.; Yu, A. C.; Chu, E. S.; Hui, A. M.; Leung, W. K. Diagnosis of gastric cancer by serum proteomic fingerprinting. *Gastroenterology* **2006**, *130*, 1858–1864.
- (33) Lu, H. B.; Zhou, J. H.; Ma, Y. Y.; Lu, H. L.; Tang, Y. L.; Zhang, Q. Y.; Zhao, C. H. Five serum proteins identified using SELDI-TOF-MS as potential biomarkers of gastric cancer. *Jpn. J. Clin. Oncol.* **2010**, *40*, 336–342.
- (34) Hao, Y.; Yu, Y.; Wang, L.; Yan, M.; Ji, J.; Qu, Y.; Zhang, J.; Liu, B.; Zhu, Z. IPO-38 is identified as a novel serum biomarker of gastric cancer based on clinical proteomics technology. *J. Proteome Res.* **2008**, *7*, 3668–3677.
- (35) Santini, D.; Vincenzi, B.; Fratto, M. E.; Perrone, G.; Lai, R.; Catalano, V.; Cass, C.; Ruffini, P. A.; Spoto, C.; Muretto, P.; Rizzo, S.; Muda, A. O.; Mackey, J. R.; Russo, A.; Tonini, G.; Graziano, F. Prognostic role of human equilibrative transporter 1 (hENT1) in patients with resected gastric cancer. *J. Cell Physiol.* **2010**, *223*, 384–388.
- (36) Oue, N.; Sentani, K.; Noguchi, T.; Ohara, S.; Sakamoto, N.; Hayashi, T.; Anami, K.; Motoshita, J.; Ito, M.; Tanaka, S.; Yoshida, K.; Yasui, W. Serum olfactomedin 4 (GW112, hGC-1) in combination with Reg IV is a highly sensitive biomarker for gastric cancer patients. *Int. J. Cancer* **2009**, *125*, 2383–2392.
- (37) Unal, B.; Kocer, B.; Altun, B.; Surmeli, S.; Aksaray, S.; Balci, M.; Ozlu, B.; Cengiz, O. Serum neopterin as a prognostic indicator in patients with gastric carcinoma. *J. Invest. Surg.* **2009**, *22*, 419–425.
- (38) Yeh, Y. C.; Sheu, B. S.; Cheng, H. C.; Wang, Y. L.; Yang, H. B.; Wu, J. J. Elevated serum matrix metalloproteinase-3 and -7 in

- H. pylori-related gastric cancer can be biomarkers correlating with a poor survival. *Dig. Dis. Sci.* **2010**, *55*, 1649–1657.
- (39) Ebert, M. P.; Krüger, S.; Fogeron, M. L.; Lamer, S.; Chen, J.; Pross, M.; Schulz, H. U.; Lage, H.; Heim, S.; Roessner, A.; Malfertheiner, P.; Röcken, C. Overexpression of cathepsin B in gastric cancer identified by proteome analysis. *Proteomics* **2005**, *5*, 1693–1704.
- (40) Liu, W.; Liu, B.; Xin, L.; Zhang, Y.; Chen, X.; Zhu, Z.; Lin, Y. Down-regulated expression of complement factor I: a potential suppressive protein for gastric cancer identified by serum proteome analysis. *Clin. Chim. Acta* **2007**, *377*, 119–126.
- (41) Jung, H.; Jun, K. H.; Jung, J. H.; Chin, H. M.; Park, W. B.. The expression of claudin-1, claudin-2, claudin-3, and claudin-4 in gastric cancer tissue. *J. Surg. Res.* **2010**, article in press, doi: 10.1016/j.jss.2010.02.010.
- (42) Zhao, Z. S.; Chu, Y. Q.; Ye, Z. Y.; Wang, Y. Y.; Tao, H. Q. Overexpression of matrix metalloproteinase 11 in human gastric carcinoma and its clinicopathologic significance. *Hum. Pathol.* **2010**, *41*, 686–696.
- (43) Kim, S. S.; Ahn, C. H.; Kang, M. R.; Kim, Y. R.; Kim, H. S.; Yoo, N. J.; Lee, S. H. Expression of CARD6, an NF- κ B activator, in gastric, colorectal and oesophageal cancers. *Pathology* **2010**, *42*, 50–53.
- (44) Zhao, Z. S.; Wang, Y. Y.; Chu, Y. Q.; Ye, Z. Y.; Tao, H. Q. SPARC is associated with gastric cancer progression and poor survival of patients. *Clin. Cancer Res.* **2010**, *16*, 260–268.
- (45) Mrena, J.; Wiksten, J. P.; Kokkola, A.; Nordling, S.; Ristimäki, A.; Haglund, C. COX-2 is associated with proliferation and apoptosis markers and serves as an independent prognostic factor in gastric cancer. *Tumor Biol.* **2010**, *31*, 1–7.
- (46) Morita, Y.; Ikegami, K.; Goto-Inoue, N.; Hayasaka, T.; Zaima, N.; Tanaka, H.; Uehara, T.; Setoguchi, T.; Sakaguchi, T.; Igarashi, H.; Sugimura, H.; Setou, M.; Konno, H. Imaging mass spectrometry of gastric carcinoma in formalin-fixed paraffin-embedded tissue microarray. *Cancer Sci.* **2010**, *101*, 267–273.
- (47) Kim, H. K.; Reyzer, M. L.; Choi, I. J.; Kim, C. G.; Kim, H. S.; Oshima, A.; Chertov, O.; Colantonio, S.; Fisher, R. J.; Allen, J. L.; Caprioli, R. M.; Green, J. E. Gastric cancer-specific protein profile identified using endoscopic biopsy samples via MALDI mass spectrometry. *J. Proteome Res.* **2010**, *9* (8), 4123–4130.
- (48) He, Q. Y.; Cheung, Y. H.; Leung, S. Y.; Yuen, S. T.; Chu, K. M.; Chiu, J. F. Diverse proteomic alterations in gastric adenocarcinoma. *Proteomics* **2004**, *4*, 3276–3287.
- (49) Li, W.; Li, J. F.; Qu, Y.; Chen, X. H.; Qin, J. M.; Gu, Q. L.; Yan, M.; Zhu, Z. G.; Liu, B. Y. Comparative proteomics analysis of human gastric cancer. *World J. Gastroenterol.* **2008**, *14*, 5657–5664.
- (50) Melle, C.; Ernst, G.; Schimmel, B.; Bleul, A.; Kaufmann, R.; Hommann, M.; Richter, K. K.; Daffner, W.; Settmacher, U.; Claussen, U.; von Eggeling, F. Characterization of pepsinogen C as a potential biomarker for gastric cancer using a histo-proteomic approach. *J. Proteome Res.* **2005**, *4*, 1799–1804.
- (51) Chen, J.; Kähne, T.; Röcken, C.; Götz, T.; Yu, J.; Sung, J. J.; Chen, M.; Hu, P.; Malfertheiner, P.; Ebert, M. P. Proteome analysis of gastric cancer metastasis by two-dimensional gel electrophoresis and matrix assisted laser desorption/ionization-mass spectrometry for identification of metastasis-related proteins. *J. Proteome Res.* **2004**, *3*, 1009–1016.
- (52) Huang, Q.; Huang, Q.; Chen, W.; Wang, L.; Lin, W.; Lin, J.; Lin, X. Identification of transgelin as a potential novel biomarker for gastric adenocarcinoma based on proteomics technology. *J. Cancer Res. Clin. Oncol.* **2008**, *134*, 1219–1227.
- (53) Yoshihara, T.; Kadota, Y.; Yoshimura, Y.; Tatano, Y.; Takeuchi, N.; Okitsu, H.; Umemoto, A.; Yamauchi, T.; Itoh, K. Proteomic alteration in gastric adenocarcinomas from Japanese patients. *Mol. Cancer* **2006**, *5*, 75–86.
- (54) Conze, T.; Carvalho, A. S.; Landegren, U.; Almeida, R.; Reis, C. A.; David, L.; Söderberg, O. MUC2 mucin is a major carrier of the cancer-associated sialyl-Tn antigen in intestinal metaplasia and gastric carcinomas. *Glycobiology* **2010**, *20*, 199–206.
- (55) Kim, Y. S.; Hwang, S. Y.; Oh, S.; Sohn, H.; Kang, H. Y.; Lee, J. H.; Cho, E. W.; Kim, J. Y.; Yoo, J. S.; Kim, N. S.; Kim, C. H.; Miyoshi, E.; Taniguchi, N.; Ko, J. H. Identification of target proteins of N-acetylglucosaminyl-transferase V and fucosyltransferase 8 in human gastric tissues by glycomic approach. *Proteomics* **2004**, *4*, 3353–3358.
- (56) Gretschel, S.; Haensch, W.; Schlag, P. M.; Kemmner, W. Clinical relevance of sialyltransferases ST6GAL-I and ST3GAL-III in gastric cancer. *Oncology* **2003**, *65*, 139–145.
- (57) Goodarzi, M. T.; Turner, G. A. Reproducible and sensitive determination of charged oligosaccharides from haptoglobin by PNGase F digestion and HPAEC/PAD analysis: glycan composition varies with disease. *Glycoconjugate J.* **1998**, *15*, 469–475.
- (58) Saldova, R.; Royle, L.; Radcliffe, C. M.; Abd Hamid, U. M.; Evans, R.; Arnold, J. N.; Banks, R. E.; Hutson, R.; Harvey, D. J.; Antrobus, R.; Petrescu, S. M.; Dwek, R. A.; Rudd, P. M. Ovarian cancer is associated with changes in glycosylation in both acute-phase proteins and IgG. *Glycobiology* **2007**, *17*, 1344–1356.
- (59) Abd Hamid, U. M.; Royle, L.; Saldova, R.; Radcliffe, C. M.; Harvey, D. J.; Storr, S. J.; Pardo, M.; Antrobus, R.; Chapman, C. J.; Zitzmann, N.; Robertson, J. F.; Dwek, R. A.; Rudd, P. M. A strategy to reveal potential glycan markers from serum glycoproteins associated with breast cancer progression. *Glycobiology* **2008**, *18*, 1105–1118.
- (60) Pierce, A.; Saldova, R.; Abd Hamid, U. M.; Abrahams, J. L.; McDermott, E. W.; Evoy, D.; Duffy, M. J.; Rudd, P. M. Levels of specific glycans significantly distinguish lymph node-positive from lymph node-negative breast cancer patients. *Glycobiology* **2010**, *20*, 1283–1288.
- (61) Alley, W. R., Jr.; Madara, M.; Mechref, Y.; Novotny, M. V. Chip-based reversed-phase liquid chromatography-mass spectrometry of permethylated N-linked glycans: a potential methodology for cancer-biomarker discovery. *Anal. Chem.* **2010**, *82*, 5095–5106.
- (62) Alley, W. R.; Novotny, M. V. Glycomics analysis of sialic acid linkages in glycans derived from blood serum glycoproteins. *J. Proteome Res.* **2010**, *9* (6), 3062–3072.
- (63) Kyselova, Z.; Mechref, Y.; Kang, P.; Goetz, J. A.; Dobrolecki, L. E.; Sledge, G. W.; Schnaper, L.; Hickey, R. J.; Malkas, L. H.; Novotny, M. V. Breast cancer diagnosis and prognosis through quantitative measurements of serum glycan profiles. *Clin. Chem.* **2008**, *54*, 1166–1175.
- (64) Royle, L.; Campbell, M. P.; Radcliffe, C. M.; White, D. M.; Harvey, D. J.; Abrahams, J. L.; Kim, Y. G.; Henry, G. W.; Shadick, N. A.; Weinblatt, M. E.; Lee, D. M.; Rudd, P. M.; Dwek, R. A. HPLC-based analysis of serum N-glycans on a 96-well plate platform with dedicated database software. *Anal. Biochem.* **2008**, *376*, 1–12.
- (65) Campbell, M. P.; Royle, L.; Radcliffe, C. M.; Dwek, R. A.; Rudd, P. M. GlycoBase and autoGU: tools for HPLC-based glycan analysis. *Bioinformatics* **2008**, *24*, 1214–1216.
- (66) Harvey, D. J.; Merry, A. H.; Royle, L.; Campbell, M. P.; Dwek, R. A.; Rudd, P. M. Proposal for a standard system for drawing structural diagrams of N- and O-linked carbohydrates and related compounds. *Proteomics* **2009**, *9*, 3796–3801.
- (67) Karp, N. A.; Lilley, K. S. Maximising sensitivity for detecting changes in protein expression: experimental design using minimal CyDyes. *Proteomics* **2005**, *5*, 3105–3115.
- (68) Karp, N. A.; Lilley, K. S. Investigating sample pooling strategies for DIGE experiments to address biological variability. *Proteomics* **2009**, *9*, 388–397.
- (69) Kang, Y.; Techanukul, T.; Mantalaris, A.; Nagy, J. M. Comparison of three commercially available DIGE analysis software packages: minimal user intervention in gel-based proteomics. *J. Proteome Res.* **2009**, *8*, 1077–1084.
- (70) Huang da, W.; Sherman, B. T.; Lempicki, R. A. Systematic and integrative analysis of large gene lists using DAVID bioinformatics resources. *Nat. Protocols* **2009**, *4*, 44–57.
- (71) Saldova, R.; Wormald, M. R.; Dwek, R. A.; Rudd, P. M. Glycosylation changes on serum glycoproteins in ovarian cancer may contribute to disease pathogenesis. *Dis. Markers* **2008**, *25*, 219–232.
- (72) Malhotra, R.; Wormald, M. R.; Rudd, P. M.; Fischer, P. B.; Dwek, R. A.; Sim, R. B. Glycosylation changes of IgG associated with

- rheumatoid arthritis can activate complement via the mannose-binding protein. *Nat. Med.* **1995**, *1*, 237–243.
- (73) Dwek, M. V.; Lacey, H. A.; Leathem, A. J. Breast cancer progression is associated with a reduction in the diversity of sialylated and neutral oligosaccharides. *Clin. Chim. Acta* **1998**, *271*, 191–202.
- (74) Krueger, K. E.; Srivastava, S. Posttranslational protein modifications: current implications for cancer detection, prevention, and therapeutics. *Mol. Cell. Proteomics* **2006**, *5*, 1799–1810.
- (75) Taylor, A. D.; Hancock, W. S.; Hincapie, M.; Taniguchi, N.; Hanash, S. M. Towards an integrated proteomic and glycomic approach to finding cancer biomarkers. *Genome Med.* **2009**, *1*, 57–68.
- (76) Hanash, S. M.; Pitteri, S. J.; Faca, V. M. Mining the plasma proteome for cancer biomarkers. *Nature* **2008**, *452*, 571–579.
- (77) An, H. J.; Miyamoto, S.; Lancaster, K. S.; Kirmiz, C.; Li, B.; Lam, K. S.; Leiserowitz, G. S.; Lebrilla, C. B. Profiling of glycans in serum for the discovery of potential biomarkers for ovarian cancer. *J. Proteome Res.* **2006**, *5*, 1626–1635.
- (78) Ravindranath, M. H.; Yesowitch, P.; Sumobay, C.; Morton, D. L. Glycoimmunomics of human cancer: current concepts and future perspectives. *Future Oncol.* **2007**, *3*, 201–214.
- (79) Kobata, A.; Amano, J. Altered glycosylation of proteins produced by malignant cells, and application for the diagnosis and immunotherapy of tumours. *Immunol. Cell Biol.* **2005**, *83*, 429–439.
- (80) Varki, N. M.; Varki, A. Diversity in cell surface sialic acid presentations: implications for biology and disease. *Lab. Invest.* **2007**, *87*, 851–857.
- (81) Seales, E. C.; Jurado, G. A.; Brunson, B. A.; Wakefield, J. K.; Frost, A. R.; Bellis, S. L. Hypersialylation of beta1 integrins, observed in colon adenocarcinoma, may contribute to cancer progression by up-regulating cell motility. *Cancer Res.* **2005**, *65*, 4645–4652.
- (82) Nordén, R.; Nyström, K.; Olofsson, S. Activation of host antiviral RNA-sensing factors necessary for herpes simplex virus type 1-activated transcription of host cell fucosyltransferase genes FUT3, FUT5, and FUT6 and subsequent expression of sLe(x) in virus-infected cells. *Glycobiology* **2009**, *19*, 776–788.
- (83) Malý, P.; Thall, A.; Petryniak, B.; Rogers, C. E.; Smith, P. L.; Marks, R. M.; Kelly, R. J.; Gersten, K. M.; Cheng, G.; Saunders, T. L.; Camper, S. A.; Camphausen, R. T.; Sullivan, F. X.; Isogai, Y.; Hindsgaul, O.; von Andrian, U. H.; Lowe, J. B. The alpha(1,3)-fucosyltransferase Fuc-TVII controls leukocyte trafficking through an essential role in L-, E-, and P-selectin ligand biosynthesis. *Cell* **1996**, *86*, 643–653.
- (84) Carvalho, A. S.; Harduin-Lepers, A.; Magalhães, A.; Machado, E.; Mendes, N.; Costa, L. T.; Matthiesen, R.; Almeida, R.; Costa, J.; Reis, C. A. Differential expression of alpha-2,3-sialyltransferases and alpha-1,3/4-fucosyltransferases regulates the levels of sialyl Lewis a and sialyl Lewis x in gastrointestinal carcinoma cells. *Int. J. Biochem. Cell Biol.* **2010**, *42*, 80–89.
- (85) Ikeguchi, M.; Hatada, T.; Yamamoto, M.; Miyake, T.; Matsunaga, T.; Fukumoto, Y.; Yamada, Y.; Fukuda, K.; Saito, H.; Tatebe, S. Serum interleukin-6 and -10 levels in patients with gastric cancer. *Gastric Cancer* **2009**, *12*, 95–100.
- (86) Delmotte, P.; Degroote, S.; Lafitte, J. J.; Lamblin, G.; Perini, J. M.; Roussel, P. Tumor necrosis factor alpha increases the expression of glycosyltransferases and sulfotransferases responsible for the biosynthesis of sialylated and/or sulfated Lewis x epitopes in the human bronchial mucosa. *J. Biol. Chem.* **2002**, *277*, 424–431.
- (87) Groux-Degroote, S.; Krzewinski-Recchi, M. A.; Cazet, A.; Vincent, A.; Lehoux, S.; Lafitte, J. J.; Van Seuningen, I.; Delannoy, P. IL-6 and IL-8 increase the expression of glycosyltransferases and sulfotransferases involved in the biosynthesis of sialylated and/or sulfated Lewis x epitopes in the human bronchial mucosa. *Biochem. J.* **2008**, *410*, 213–223.
- (88) Kim, Y. J.; Varki, A. Perspectives on the significance of altered glycosylation of glycoproteins in cancer. *Glycoconjugate J.* **1997**, *14*, 569–576.
- (89) Ono, M.; Hakomori, S. Glycosylation defining cancer cell motility and invasiveness. *Glycoconjugate J.* **2004**, *20*, 71–78.
- (90) Amado, M.; Carneiro, F.; Seixas, M.; Clausen, H.; Sobrinho-Simões, M. Dimeric sialyl-Le(x) expression in gastric carcinoma correlates with venous invasion and poor outcome. *Gastroenterology* **1998**, *114*, 462–470.
- (91) Koike, T.; Kimura, N.; Miyazaki, K.; Yabuta, T.; Kumamoto, K.; Takenoshita, S.; Chen, J.; Kobayashi, M.; Hosokawa, M.; Taniguchi, A.; Kojima, T.; Ishida, N.; Kawakita, M.; Yamamoto, H.; Takematsu, H.; Suzuki, A.; Kozutsumi, Y.; Kannagi, R. Hypoxia induces adhesion molecules on cancer cells: A missing link between Warburg effect and induction of selectin-ligand carbohydrates. *Proc. Natl. Acad. Sci. U.S.A.* **2004**, *101*, 8132–8137.
- (92) Axford, J. S.; Sumar, N.; Alavi, A.; Isenberg, D. A.; Young, A.; Bodman, K. B.; Roitt, I. M. Changes in normal glycosylation mechanisms in autoimmune rheumatic disease. *J. Clin. Invest.* **1992**, *89*, 1021–1031.
- (93) Omtvedt, L. A.; Royle, L.; Husby, G.; Sletten, K.; Radcliffe, C. M.; Harvey, D. J.; Dwek, R. A.; Rudd, P. M. Glycan analysis of monoclonal antibodies secreted in deposition disorders indicates that subsets of plasma cells differentially process IgG glycans. *Arthritis Rheum.* **2006**, *54*, 3433–3440.
- (94) Arnold, J. N.; Dwek, R. A.; Rudd, P. M.; Sim, R. B. Mannan binding lectin and its interaction with immunoglobulins in health and in disease. *Immunol. Lett.* **2006**, *106*, 103–110.
- (95) Arnold, J. N.; Wormald, M. R.; Sim, R. B.; Rudd, P. M.; Dwek, R. A. The impact of glycosylation on the biological function and structure of human immunoglobulins. *Annu. Rev. Immunol.* **2007**, *25*, 21–50.
- (96) Kanoh, Y.; Mashiko, T.; Danbara, M.; Takayama, Y.; Ohtani, S.; Imasaki, T.; Abe, T.; Akahoshi, T. Analysis of the oligosaccharide chain of human serum immunoglobulin g in patients with localized or metastatic cancer. *Oncology* **2004**, *66*, 365–370.
- (97) Bereman, M. S.; Muddiman, D. C. The effects of abundant plasma protein depletion on global glycan profiling using nanoLC FT-ICR mass spectrometry. *Anal. Bioanal. Chem.* **2010**, *396*, 1473–1479.
- (98) He, Z.; Aristoteli, L. P.; Krishnadas, L.; Garner, B. HPLC analysis of discrete haptoglobin isoform N-linked oligosaccharides following 2D-PAGE isolation. *Biochem. Biophys. Res. Commun.* **2006**, *343*, 496–503.
- (99) Ang, I. L.; Poon, T. C.; Lai, P. B.; Chan, A. T.; Ngai, S. M.; Hui, A. Y.; Johnson, P. J.; Sung, J. J. Study of serum haptoglobin and its glycoforms in the diagnosis of hepatocellular carcinoma: a glycoproteomic approach. *J. Proteome Res.* **2006**, *5*, 2691–2700.
- (100) Hoagland, L. F., IV; Campa, M. J.; Gottlin, E. B.; Herndon, J. E., II; Patz, E. F., Jr. Haptoglobin and posttranslational glycan-modified derivatives as serum biomarkers for the diagnosis of nonsmall cell lung cancer. *Cancer* **2007**, *110*, 2260–2268.
- (101) Miyoshi, E.; Nakano, M. Fucosylated haptoglobin is a novel marker for pancreatic cancer: detailed analyses of oligosaccharide structures. *Proteomics* **2008**, *8*, 3257–3262.
- (102) Okuyama, N.; Ide, Y.; Nakano, M.; Nakagawa, T.; Yamanaka, K.; Moriwaki, K.; Murata, K.; Ohigashi, H.; Yokoyama, S.; Eguchi, H.; Ishikawa, O.; Ito, T.; Kato, M.; Kasahara, A.; Kawano, S.; Gu, J.; Taniguchi, N.; Miyoshi, E. Fucosylated haptoglobin is a novel marker for pancreatic cancer: a detailed analysis of the oligosaccharide structure and a possible mechanism for fucosylation. *Int. J. Cancer* **2006**, *118*, 2803–2808.
- (103) Sarrats, A.; Saldova, R.; Pla, E.; Fort, E.; Harvey, D. J.; Struwe, W. B.; de Llorens, R.; Rudd, P. M.; Peracaula, R. Glycosylation of liver acute-phase proteins in pancreatic cancer and chronic pancreatitis. *Proteomics: Clin. Appl.* **2010**, *4*, 432–448.
- (104) Nakano, M.; Nakagawa, T.; Ito, T.; Kitada, T.; Hijioka, T.; Kasahara, A.; Tajiri, M.; Wada, Y.; Taniguchi, N.; Miyoshi, E. Site-specific analysis of N-glycans on haptoglobin in sera of patients with pancreatic cancer: a novel approach for the development of tumor markers. *Int. J. Cancer* **2008**, *122*, 2301–2309.
- (105) Narisada, M.; Kawamoto, S.; Kuwamoto, K.; Moriwaki, K.; Nakagawa, T.; Matsumoto, H.; Asahi, M.; Koyama, N.; Miyoshi, E. Identification of an inducible factor secreted by pancreatic cancer cell

lines that stimulates the production of fucosylated haptoglobin in hepatoma cells. *Biochem. Biophys. Res. Commun.* **2008**, *377*, 792–796.

(106) Jenne, D. E.; Tschopp, J.. Clusterin: the intriguing guises of a widely expressed glycoprotein. *Trends Biochem. Sci.* **1992**, *17*, 154–159.

(107) Tschopp, J.; French, L. E. Clusterin: modulation of complement function. *Clin. Exp. Immunol.* **1994**, *97*, 11–14.

(108) Shannan, B.; Seifert, M.; Leskov, K.; Willis, J.; Boothman, D.; Tilgen, W.; Reichrath, J. Challenge and promise: roles for clusterin in pathogenesis, progression and therapy of cancer. *Cell Death Differ.* **2006**, *13*, 12–19.

(109) Andersen, C. L.; Schepeler, T.; Thorsen, K.; Birkenkamp-Demtroder, K.; Mansilla, F.; Aaltonen, L. A.; Laurberg, S.; Ørntoft, T. F. Clusterin expression in normal mucosa and colorectal cancer. *Mol. Cell. Proteomics* **2007**, *6*, 1039–1048.

(110) Zoubeidi, A.; Ettinger, S.; Beraldi, E.; Hadaschik, B.; Zardan, A.; Klomp, L. W.; Nelson, C. C.; Rennie, P. S.; Gleave, M. E. Clusterin facilitates COMMD1 and I-kappaB degradation to enhance NF-kappaB activity in prostate cancer cells. *Mol. Cancer Res.* **2010**, *8*, 119–130.

(111) Kakisaka, T.; Kondo, T.; Okano, T.; Fujii, K.; Honda, K.; Endo, M.; Tsuchida, A.; Aoki, T.; Itoi, T.; Moriyasu, F.; Yamada, T.; Kato, H.; Nishimura, T.; Todo, S.; Hirohashi, S. Plasma proteomics of pancreatic cancer patients by multi-dimensional liquid chromatography and two-dimensional difference gel electrophoresis (2D-DIGE): up-regulation of leucine-rich alpha-2-glycoprotein in pancreatic cancer. *J. Chromatogr., B* **2007**, *852*, 257–267.

(112) Shirai, R.; Hirano, F.; Ohkura, N.; Ikeda, K.; Inoue, S. Up-regulation of the expression of leucine-rich alpha(2)-glycoprotein in hepatocytes by the mediators of acute-phase response. *Biochem. Biophys. Res. Commun.* **2009**, *382*, 776–779.

(113) Cummings, C.; Walder, J.; Treeful, A.; Jemmerson, R. Serum leucine-rich alpha-2-glycoprotein-1 binds cytochrome c and inhibits antibody detection of this apoptotic marker in enzyme-linked immunosorbent assay. *Apoptosis* **2006**, *11*, 1121–1129.

(114) Codina, R.; Vanasse, A.; Kelekar, A.; Vezys, V.; Jemmerson, R. Cytochrome c-induced lymphocyte death from the outside in: inhibition by serum leucine-rich alpha-2-glycoprotein-1. *Apoptosis* **2010**, *15*, 139–152.

(115) Qiu, Y.; Patwa, T. H.; Xu, L.; Shedden, K.; Misek, D. E.; Tuck, M.; Jin, G.; Ruffin, M. T.; Turgeon, D. K.; Synal, S.; Bresalier, R.; Marcon, N.; Brenner, D. E.; Lubman, D. M. Plasma glycoprotein profiling for colorectal cancer biomarker identification by lectin glycoarray and lectin blot. *J. Proteome Res.* **2008**, *7*, 1693–1703.

(116) Barbasz, A.; Guevara-Lora, I.; Rapala-Kozik, M.; Kozik, A. Kininogen binding to the surfaces of macrophages. *Int. Immunopharmacol.* **2008**, *8*, 211–216.